Supporting Information

Nickel(II) PE^1CE^2P pincer complexes (E = O, S) for electrocatalytic proton reduction

Sandeep Kaur-Ghumaan[a,b]*, Patrick Hasche[a], Anke Spannenberg[a], and Torsten Beweries[a]*

[a]Leibniz-Institut für Katalyse e.V. an der Universität Rostock, Albert-Einstein-Str. 29a, 18059 Rostock, Germany, Email: torsten.beweries@catalysis.de

[b] Department of Chemistry, University of Delhi (North Campus), New Delhi-110007, India

Email: skaur@chemistry.du.ac.in, torsten.beweries@catalysis.de

Table of contents

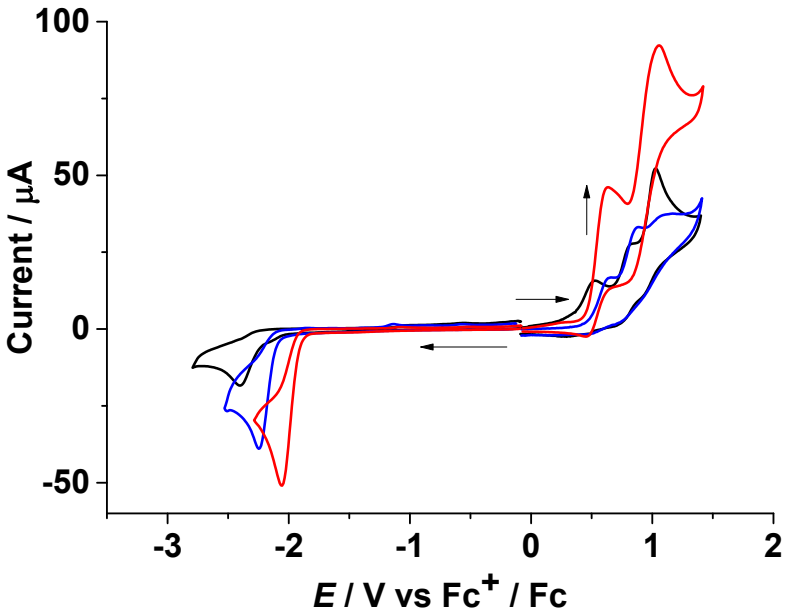

Figure S1. CVs (under argon) for complexes **1** (1 mM) (black), **2** (1.47 mM) (blue) and **3** (1.43 mM) (red) in the absence of acid in MeCN with 0.1 M TBAP at a scan rate of 0.1 V /s.

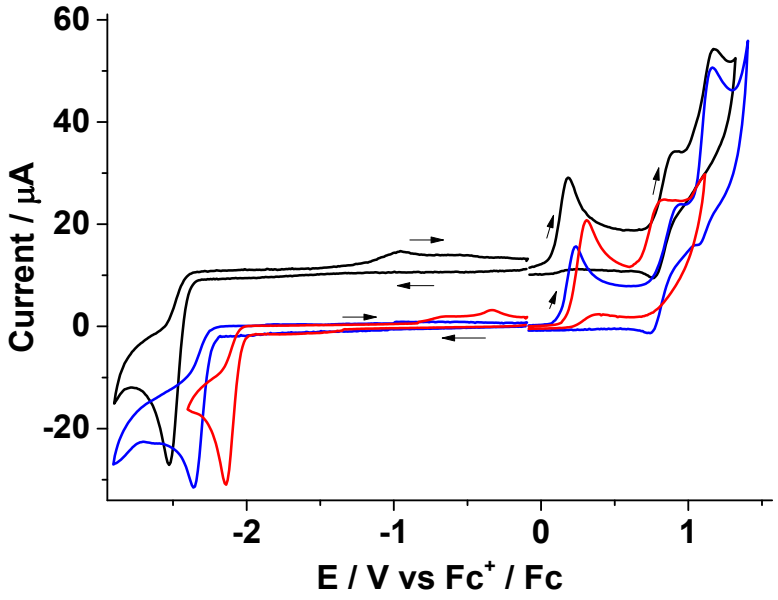

Figure S2. CVs (under argon) for complexes **4** (1.15 mM) (black), **5** (0.93 mM) (blue) and **6** (1 mM) (red) in the absence of acid in MeCN with 0.1 M TBAP at a scan rate of 0.1 V /s.

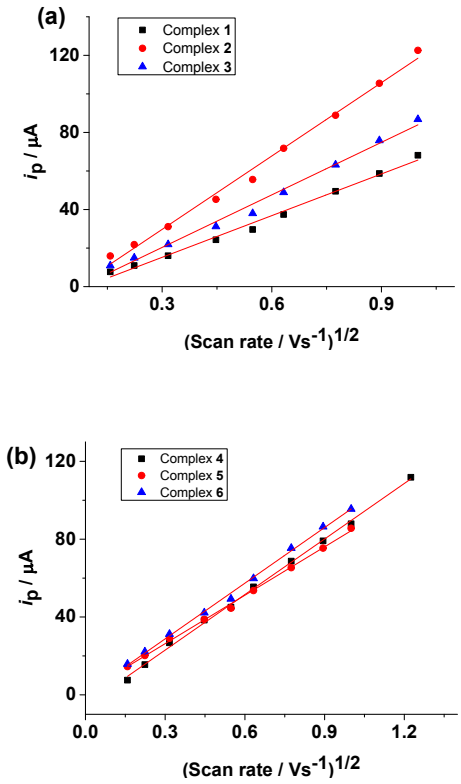

Figure S3. Plot of current (i_p) *vs*. (scan rate (ν))$^{1/2}$ (0.025-1 Vs^{-1}) for the reduction peaks of (a) complexes **1** (black) (0.5 mM), **2** (red) (1.11 mM) and **3** (blue) (1.07 mM) and (b) complexes **4** (black) (1.15 mM), **5** (red) (0.93 mM) and **6** (blue) (1 mM). Lines are best fit lines to the data. Linear plot of i_p vs square root of the scan rate suggests no deposition of the catalyst on the electrode surface.

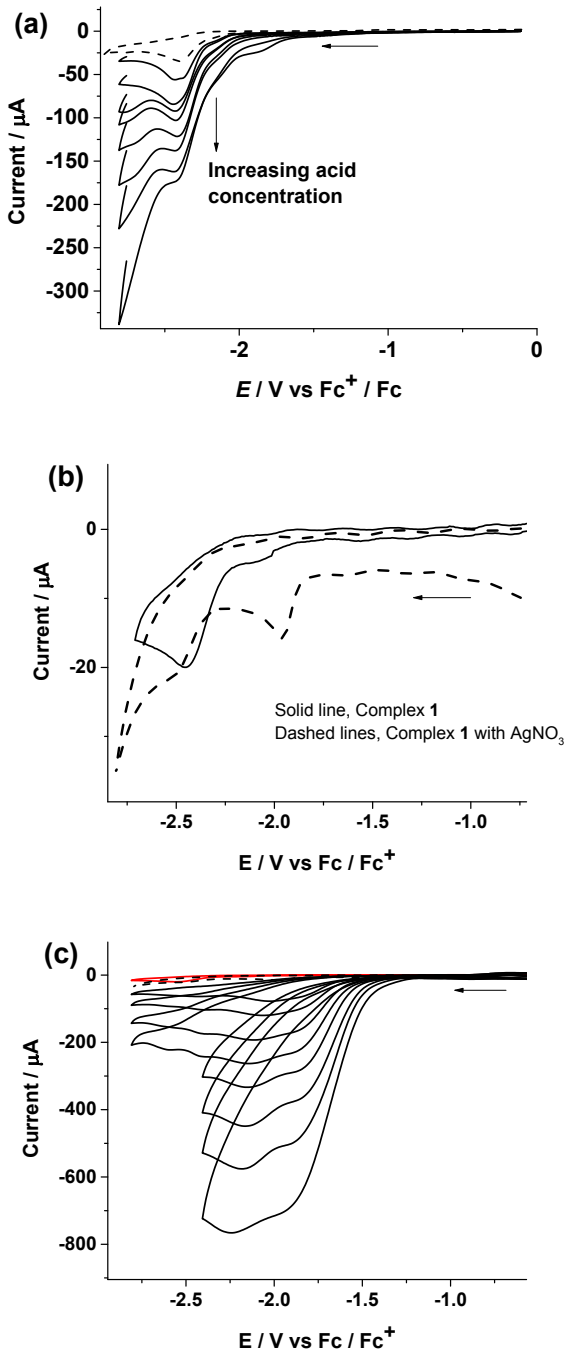

Figure S4. (a) CVs (under argon) for complex **1** (1 mM) in MeCN in the absence (---) and presence of (0.97, 2.90, 4.82, 6.75, 10.58, 18.20, 25.74, 40.64 mM) (**—**) acetic acid with 0.1 M TBAP at 0.1 V /s. The reverse scans have been omitted for clarity. (b) CVs (under argon) for complex **1** (0.46 mM) in MeCN in the absence (**—**) and presence (---) of $AgNO_3$ at 0.1 V/s. (c) CVs (under argon) for complex **1** (0.46 mM) in MeCN in the absence (---) and presence of (0-82 mM) (**—**) acetic acid with 0.1 M TBAP at 0.1 V /s. CVs with acetic acid were measured after addition of $AgNO_3$ to the MeCN solution of the sample.

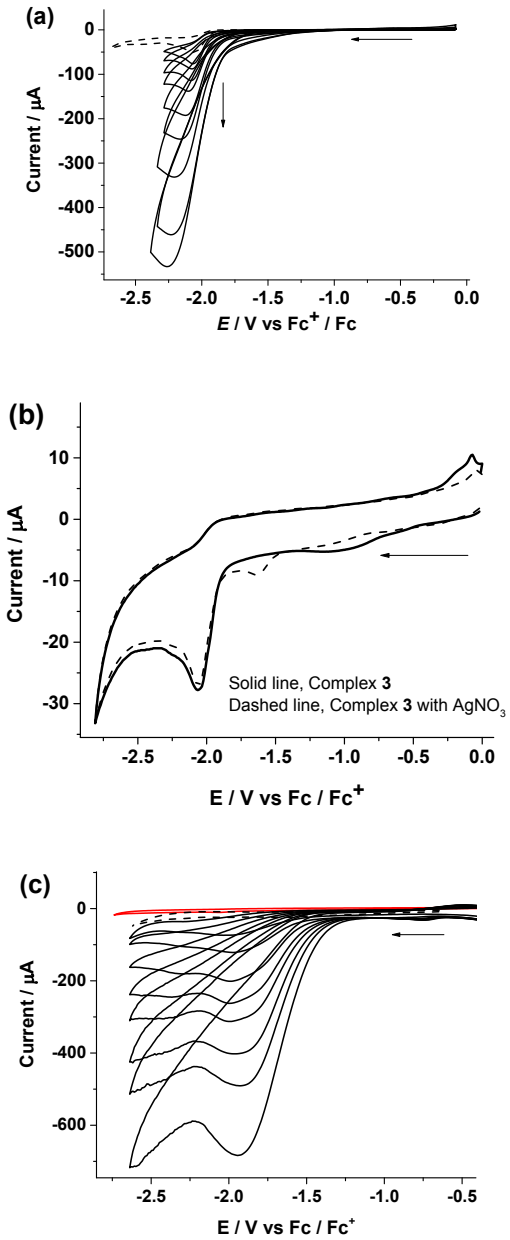

Figure S5. (a) CVs for [$^{i\text{Pr}}$PSCSP$^{i\text{Pr}}$]NiCl (**3**) (1.43 mM) in MeCN in the absence (---) and presence of (1.35, 2.71, 5.40, 8.09, 13.44, 18.76, 29.31, 39.72, 50 mM) (—) of acetic acid at 0.1 V /s. (b) CVs (under argon) for complex **3** (0.43 mM) in MeCN in the absence (—) and presence (---) of $AgNO_3$ at 0.1 V/s. (c) CVs (under argon) for complex **3** (0.43 mM) in MeCN in the absence (---) and presence of (0-28 mM) (—) acetic acid with 0.1 M TBAP at 0.1 V /s. CVs with acetic acid were measured after addition of $AgNO_3$ to the MeCN solution of the sample.

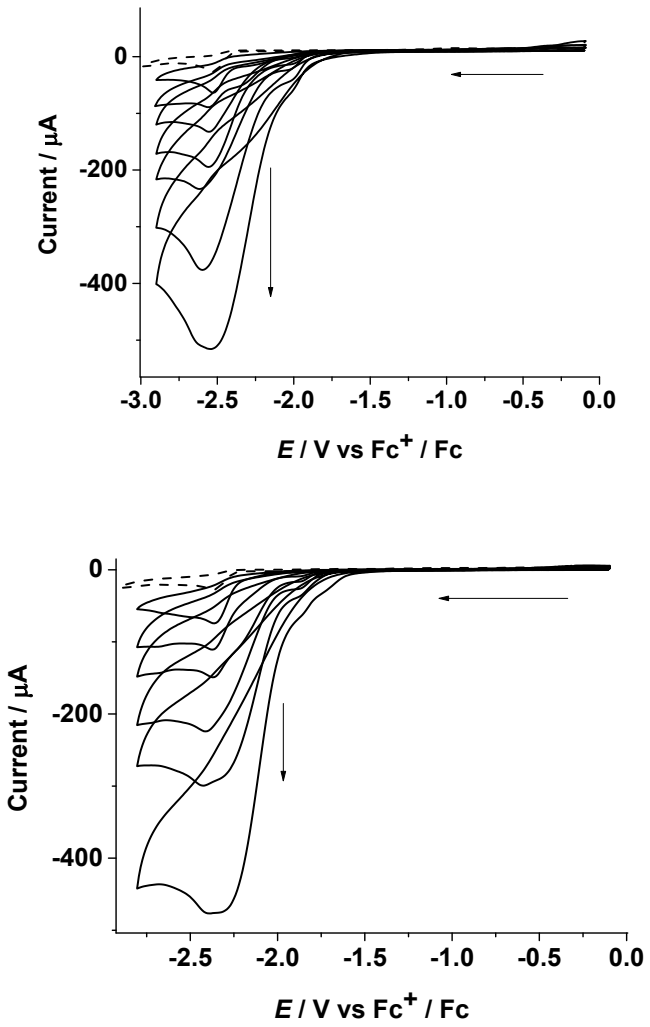

Figure S6. Top: CVs for [$^{i\text{Pr}}$POCOP$^{i\text{Pr}}$]NiSC$_6$H$_4$CH$_3$ (**4**) (1.15 mM) in MeCN in the absence (---) and presence of (2.61, 6.076, 9.53, 16.39, 23.2, 36.66, 49.92 mM) (**—**) of acetic acid at 0.1 V /s. Bottom: CVs for [$^{i\text{Pr}}$POCSP$^{i\text{Pr}}$]NiSC$_6$H$_4$CH$_3$ (**5**) (0.93 mM) in MeCN in the absence (---) and presence of (2.61, 6.075, 9.53, 16.39, 23.203, 36.66 mM) (**—**) of acetic acid at 0.1 V /s.

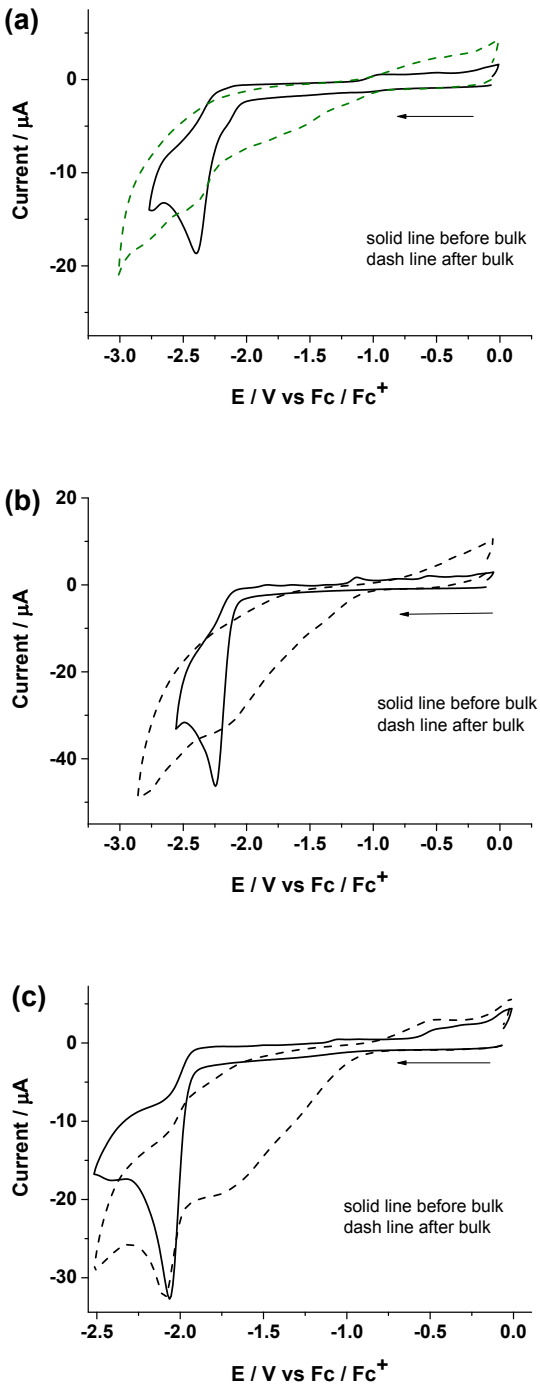

Figure S7. CVs for 1 mM (a) complex **1**, (b) complex **2** and (c) complex **3** in MeCN before and after bulk electrolysis experiment with 0.1 M TBAP at 0.1 V /s. Bulk electrolysis was carried out at the first reduction potential of the complexes.

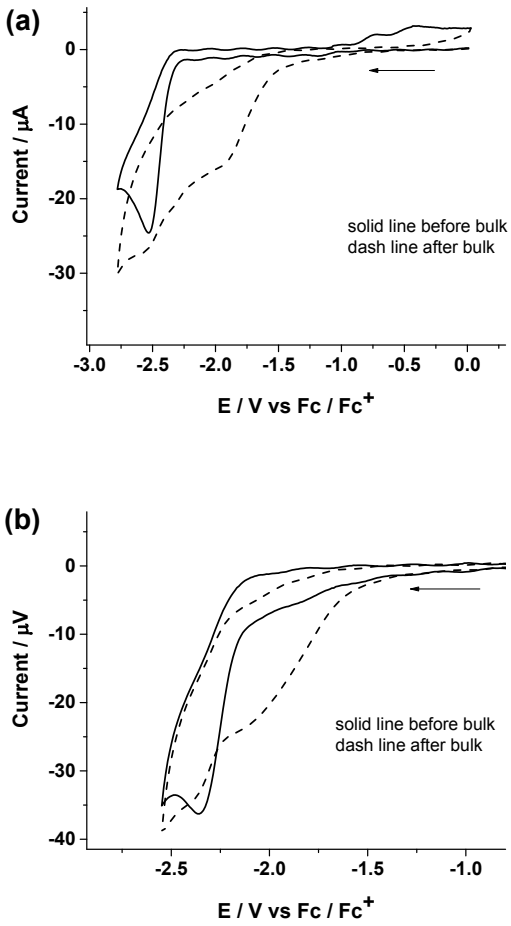

Figure S8. CVs for 0.5 mM (a) complex **4** and (b) complex **5** in MeCN before and after bulk electrolysis experiment with 0.1 M TBAP at 0.1 V /s. Bulk electrolysis was carried out at the first reduction potential of the complexes.

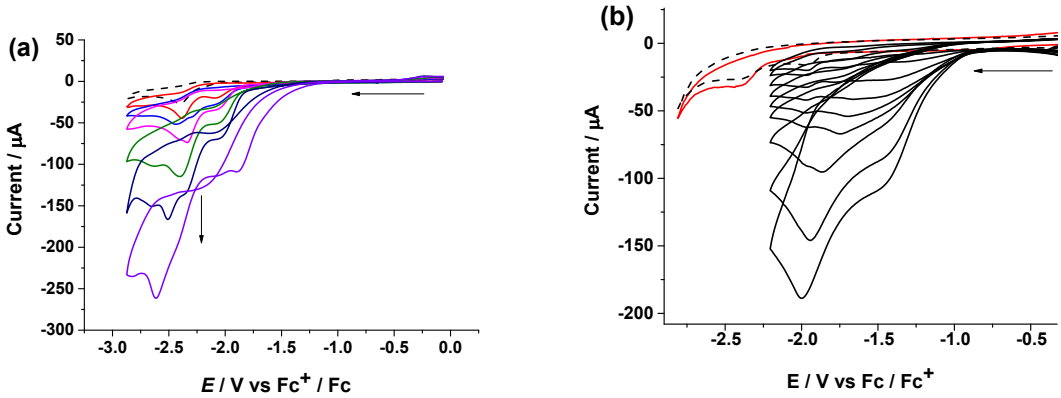

Figure S9. (a) CVs (under argon) for complex **1** (1.02 mM) in MeCN in the absence (---) and presence of (0.66, 1.33, 1.99, 3.97, 5.94, 9.84 mM) (—) of TFA with 0.1 M TBAP at 0.1 V /s. (b) CVs (under argon) for complex **1** (0.46 mM) in MeCN in the absence (---) and presence of (0-5 mM) (—) of TFA with 0.1 M TBAP at 0.1 V /s. CVs with TFA were measured after addition of $AgNO_3$ to the MeCN solution of the sample.

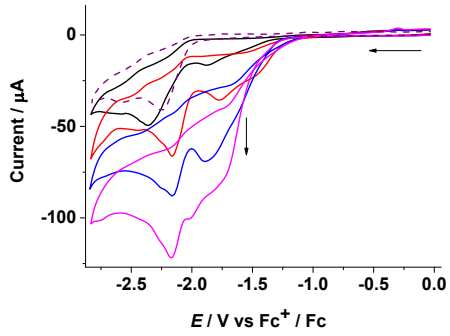

Figure S10. CVs (under argon) for complex **2** (1.11 mM) in MeCN in the absence (---) and presence of (0.60, 1.19, 2.39, 3.58 mM) (—) of TFA with 0.1 M TBAP at 0.1 V /s.

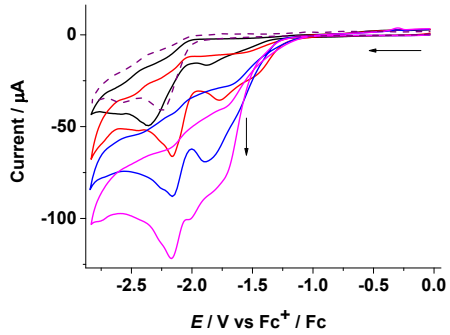

Figure S11. CVs (under argon) for complex **3** (1.87 mM) in MeCN in the absence (---) and presence of (0.75, 1.50, 2.99, 4.47, 5.94 mM) (—) of TFA with 0.1 M TBAP at 0.1 V /s.

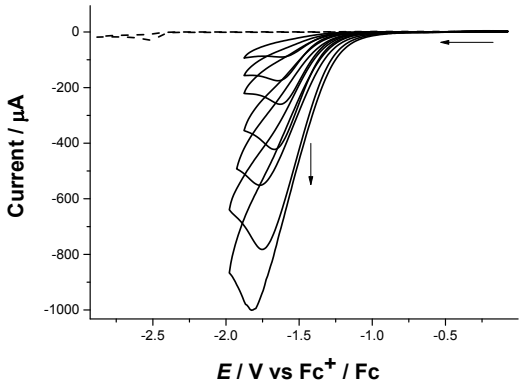

Figure S12. CVs (under argon) for [$^{i\text{Pr}}$POCOP$^{i\text{Pr}}$]NiSC$_6$H$_4$CH$_3$ (**4**) (0.85 mM) in MeCN in the absence (---) and presence of (6.59, 11.76, 14.32, 24.31, 33.96, 47.85, 61.08 mM) (—) of TFA with 0.1 M TBAP at 0.1 V /s.

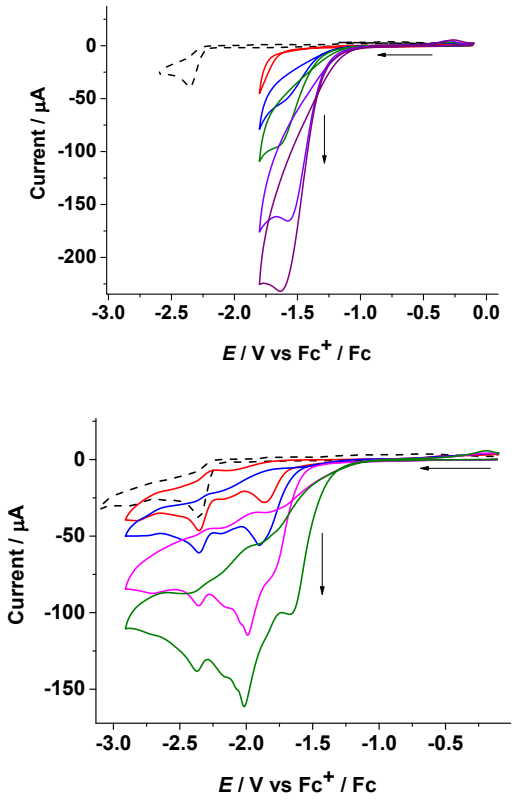

Figure S13. CVs (under argon) for complex **5** (1.24 mM) in MeCN in the absence (---) and presence of (1.99, 3.97, 5.94, 9.84, 13.68 mM) (—) of TFA with 0.1 M TBAP at 0.1 V /s.

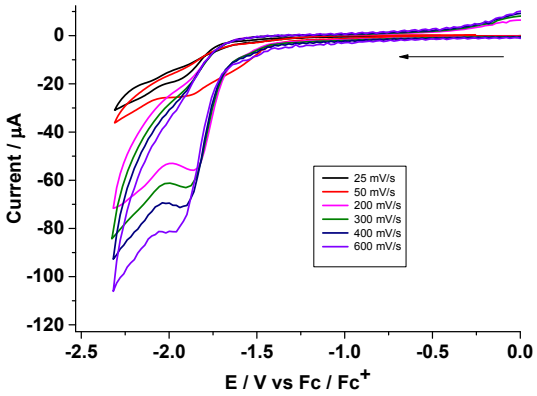

Figure S14. CVs (under argon) for complex **1** (0.5 mM) in MeCN in the presence of AA at different scan rates.

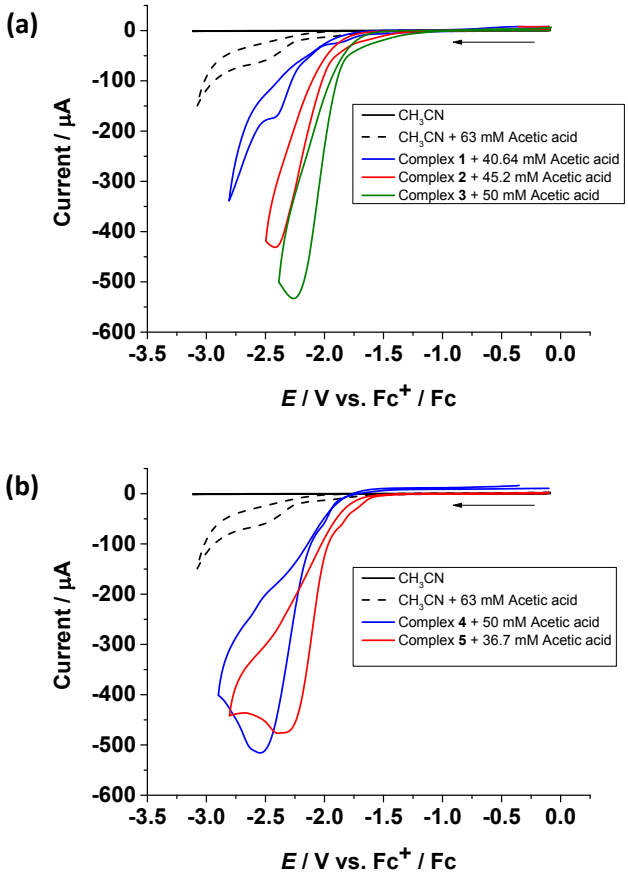

Figure S15. (a) CVs (0.1 Vs^{-1}) of CH_3CN (——), of CH_3CN and 63 mM acetic acid (- - -), of [^{iPr}POCOP^{iPr}]NiCl (**1**) (1 mM) (——) in the presence of 40.64 mM of acetic acid, of [^{iPr}POCSP^{iPr}]NiCl (**2**) (1.47 mM) (——) in the presence of 45.2 mM of acetic acid and of [^{iPr}PSCSP^{iPr}]NiCl (**3**) (1.43 mM) (——) in the presence of 50 mM of acetic acid in CH_3CN. (b) CVs (0.1 Vs^{-1}) of CH_3CN (——), of CH_3CN and 63 mM acetic acid (- - -), of [^{iPr}POCOP^{iPr}]NiSC$_6$H$_4$CH$_3$ (**4**) (1.15 mM) (——) in the presence of 50 mM of acetic acid and of [^{iPr}POCSP^{iPr}]NiSC$_6$H$_4$CH$_3$ (**5**) (1.15 mM) (——) in the presence of 36.7 mM of acetic acid in CH_3CN.

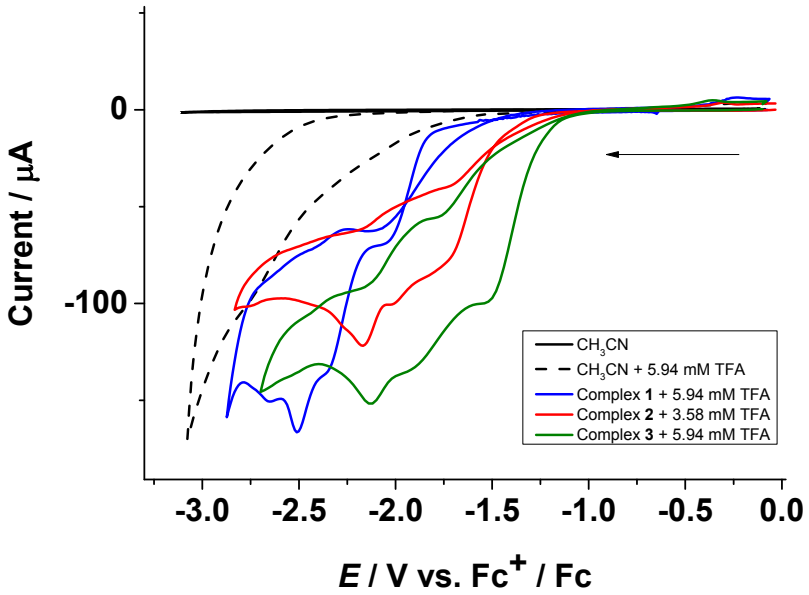

Figure S16. CVs (0.1 Vs^{-1}) of CH_3CN (——), of CH_3CN and 5.94 mM TFA (- - -), of [$^{i\text{Pr}}$POCOP$^{i\text{Pr}}$]NiCl (**1**) (1.02 mM) (——) in the presence of 5.94 mM of TFA, of [$^{i\text{Pr}}$POCSP$^{i\text{Pr}}$]NiCl (**2**) (1.11 mM) (——) in the presence of 3.58 mM of TFA and of [$^{i\text{Pr}}$PSCSP$^{i\text{Pr}}$]NiCl (**3**) (1.87 mM) (——) in the presence of 5.94 mM of TFA in CH_3CN.

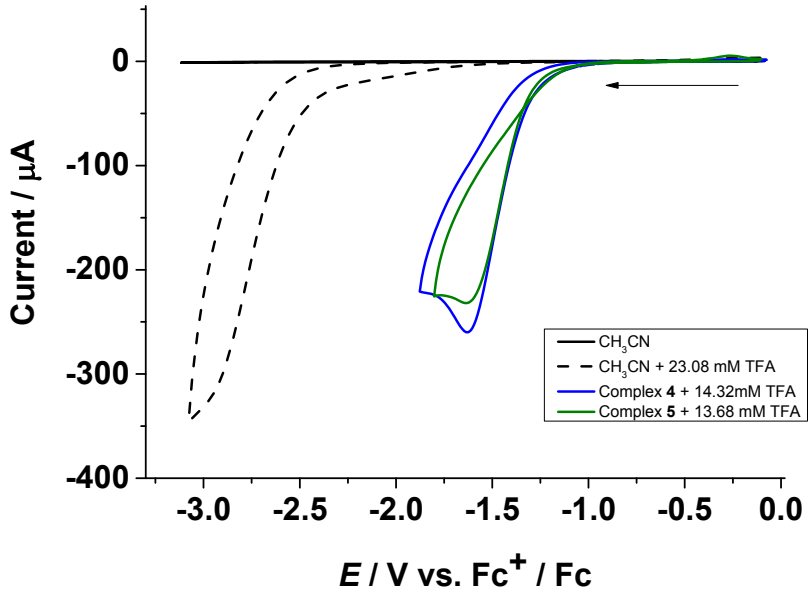

Figure S17. CVs (0.1 Vs^{-1}) of CH_3CN (——), of CH_3CN and 23.08 mM TFA (- - -), of [$^{i\text{Pr}}$POCOP$^{i\text{Pr}}$]Ni$SC_6H_4CH_3$ (**4**) (0.85 mM) (——) in the presence of 14.32 mM of TFA and of [$^{i\text{Pr}}$POCSP$^{i\text{Pr}}$]Ni$SC_6H_4CH_3$ (**5**) (1.24 mM) (——) in the presence of 13.68 mM of TFA in CH_3CN.

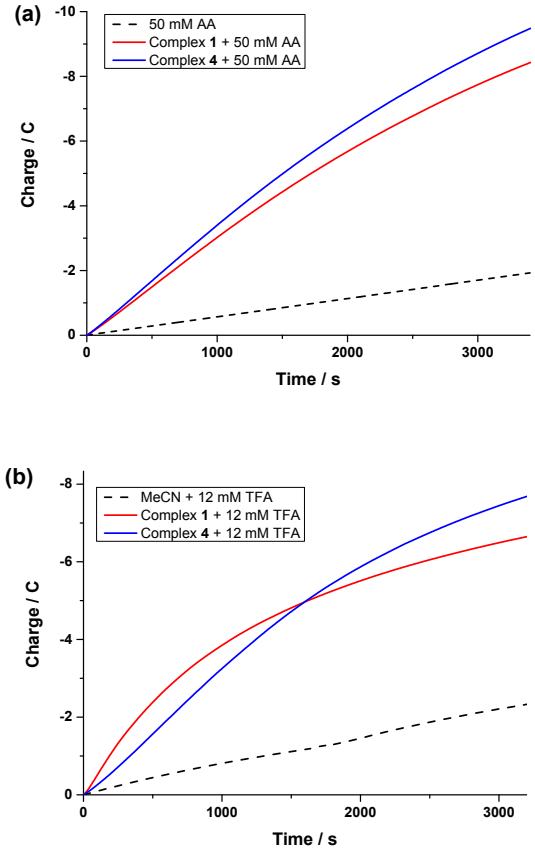

Figure S18. Plot of charge *vs.* time for controlled-potential electrolysis of 1 mM complexes **1** and **4** (a) with AA (-2.4/-2.5 V) and (b) with TFA at -1.9/-1.8 V in CH_3CN / 0.1 M $[N(n\text{-}Bu_4)][PF_6]$.

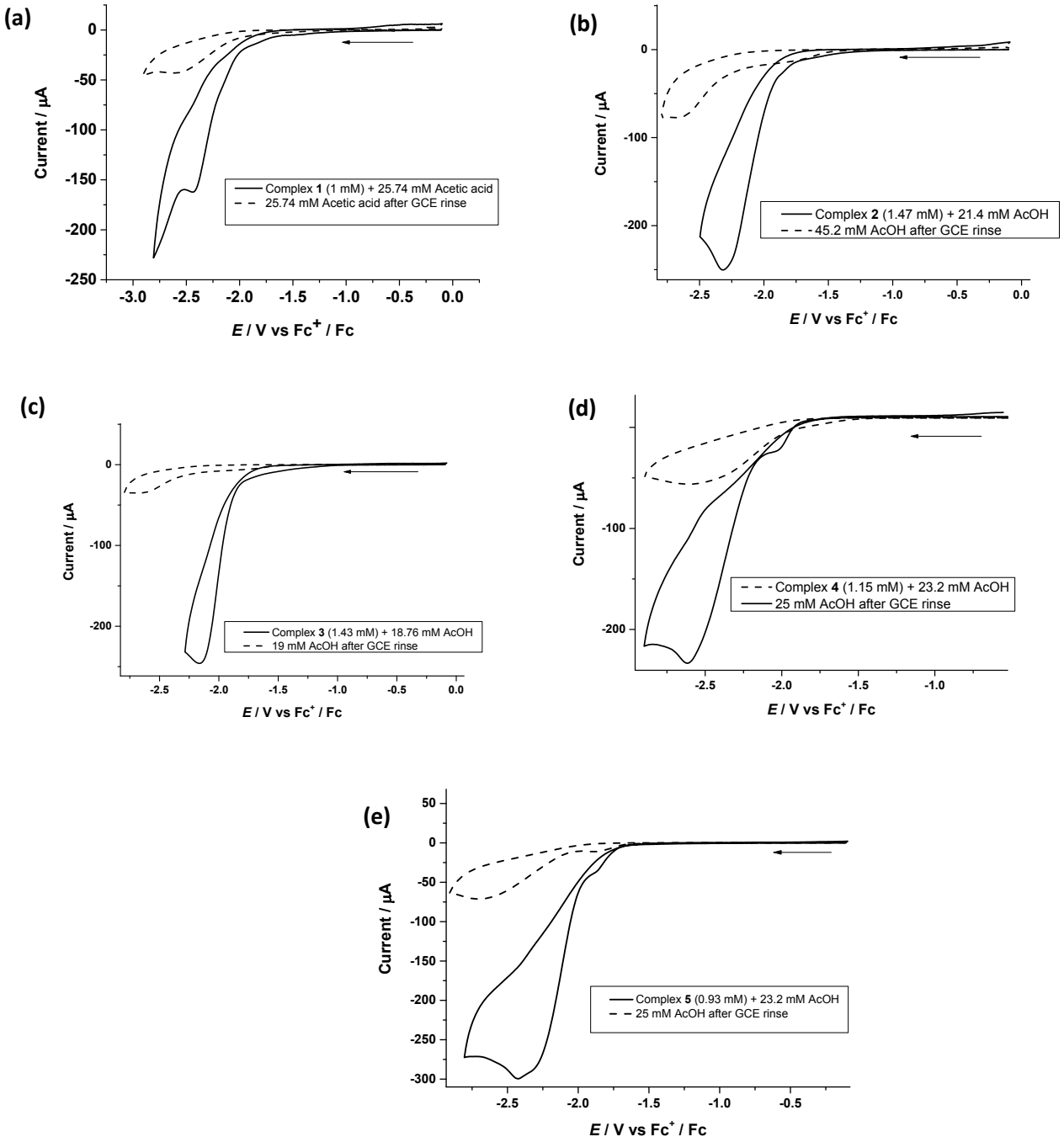

Figure S19. Rinse test was performed with the [$^{i\text{Pr}}$PE^{1}CE^{2}P$^{i\text{Pr}}$]NiCl (**1**-**3**) and [$^{i\text{Pr}}$PE^{1}CE^{2}P$^{i\text{Pr}}$]NiSC$_6$H$_4$CH$_3$ (**4** and **5**) complexes. The solid black line is for catalysis in the presence of the catalysts with acetic acid at 0.1 Vs^{-1}. The working electrode (GCE) was then dipped into the solution having the same amount of acetic acid but without the catalyst after gently rinsing with acetonitrile (black dashed line) at 0.1 Vs^{-1}. The Pt counter and Ag/AgCl reference electrodes were also cleaned thoroughly before the rinse test.

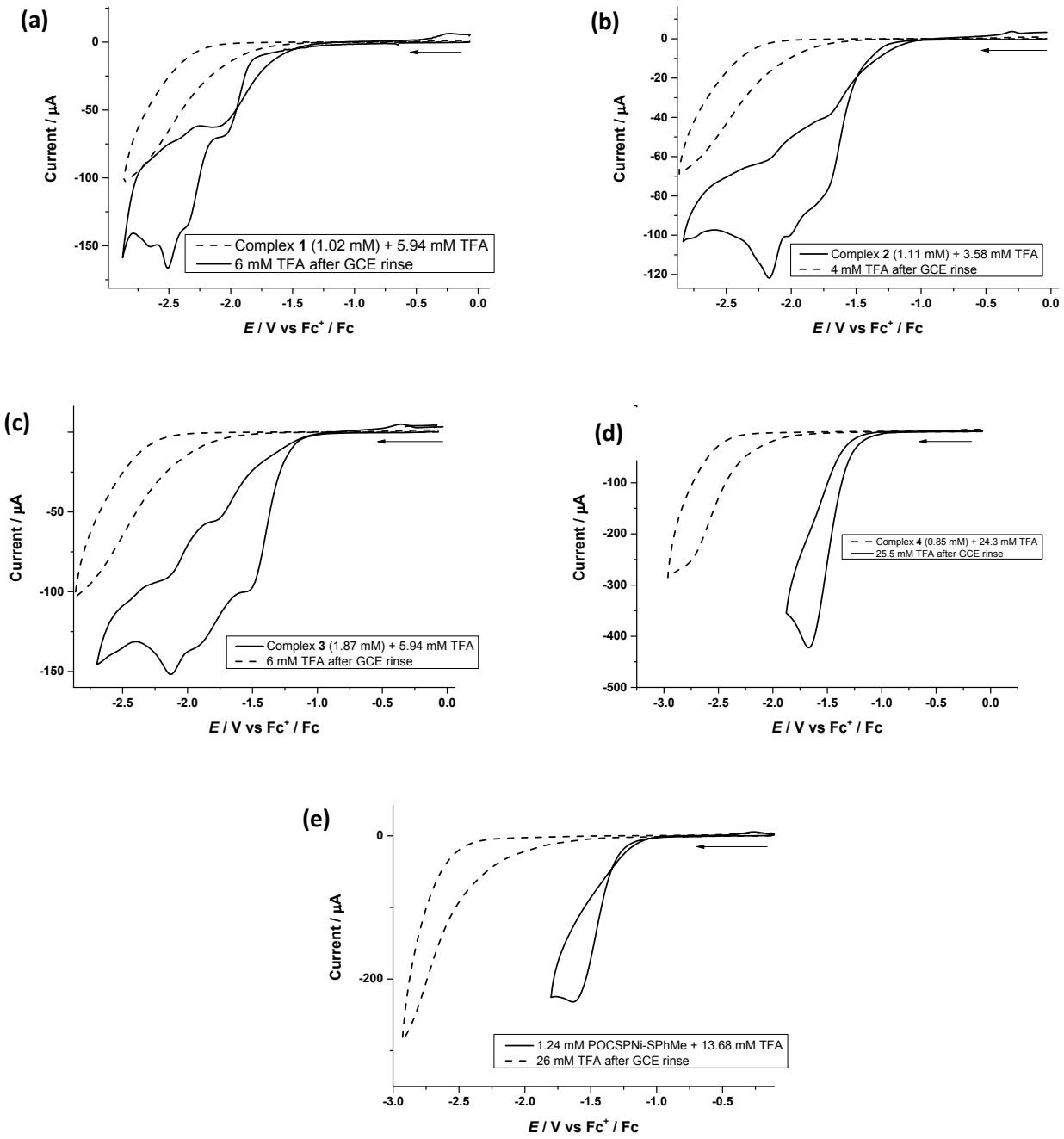

Figure S20. Rinse test was performed with the [$^{i\text{Pr}}$PE^{1}CE^{2}P$^{i\text{Pr}}$]NiCl (**1**-**3**) and the [$^{i\text{Pr}}$PE^{1}CE^{2}P$^{i\text{Pr}}$]NiSC$_6$H$_4$CH$_3$ (**4** and **5**) complexes. The solid black line is for catalysis in the presence of the catalysts with TFA at 0.1 Vs^{-1}. The working electrode (GCE) was then dipped into the solution having the same amount of TFA but without the catalyst after gently rinsing with acetonitrile (black dashed line) at 0.1 Vs^{-1}. The Pt counter and Ag/AgCl reference electrodes were also cleaned thoroughly before the rinse test.

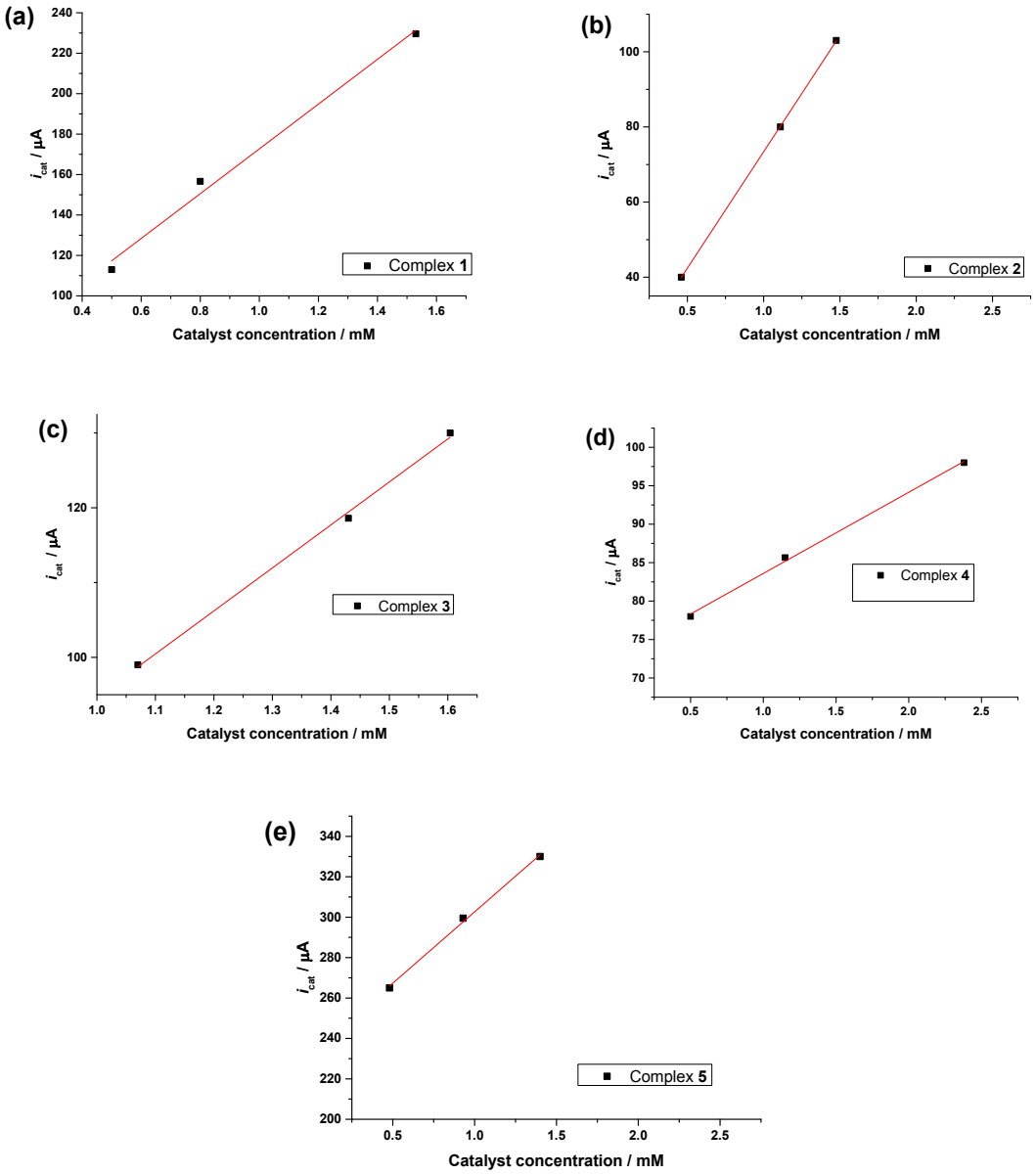

Figure S21. i_{cat} vs catalyst concentration plots for (a) [$^{i\text{Pr}}$POCOP$^{i\text{Pr}}$]NiCl (**1**) with acetic acid (26 mM), (b) for [$^{i\text{Pr}}$POCSP$^{i\text{Pr}}$]NiCl (**2**) with acetic acid (6.17 mM), (c) for [$^{i\text{Pr}}$PSCSP$^{i\text{Pr}}$]NiCl (**3**) with acetic acid (6.51 mM), (d) for [$^{i\text{Pr}}$POCOP$^{i\text{Pr}}$]NiSC$_6$H$_4$CH$_3$ (**4**) with acetic acid (4.34 mM) and (e) for [$^{i\text{Pr}}$POCSP$^{i\text{Pr}}$]NiSC$_6$H$_4$CH$_3$ (**5**) with acetic acid (23.2 mM) in MeCN with 0.1 M TBAP at 0.1 V/s. Lines are the best-linear fit to the data.

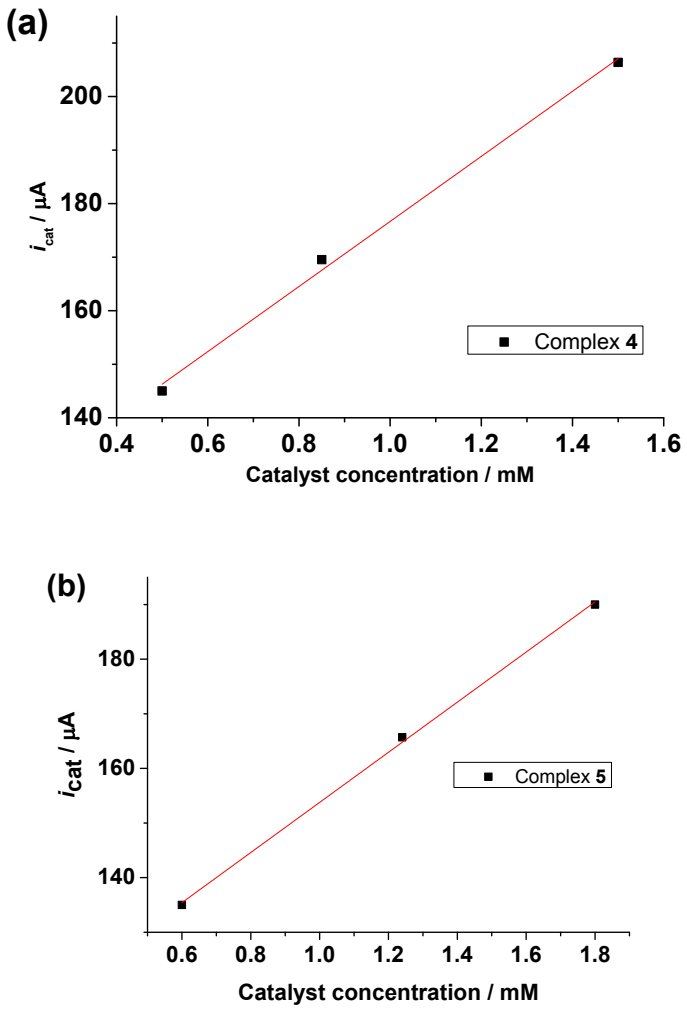

Figure S22. i_{cat} vs catalyst concentration plots for (a) for [$^{i\text{Pr}}$POCOP$^{i\text{Pr}}$]NiSC$_6$H$_4$CH$_3$ (**4**) with TFA (14.32 mM) and (b) for [$^{i\text{Pr}}$POCSP$^{i\text{Pr}}$]NiSC$_6$H$_4$CH$_3$ (**5**) with TFA (9.84 mM) in MeCN with 0.1 M TBAP at 0.1 V/s. Lines are the best-linear fit to the data.

Proton reduction kinetics:

For a diffusion limited catalytic process that occurs at high enough [H^+] that the concentration remains unchanged, the observed current obeys the following equation:

$i_{cat} = nFA\,[cat]\sqrt{Dk[H^+]^2}$ **(1)**

The peak current observed in the absence of acid for the complex, can be written as:

$i_p = 0.443FA\,[cat]\sqrt{\frac{F\nu D}{RT}}$ **(2)**

Dividing (**1**) by (**2**), results in the following expression:

$$\frac{i_{cat}}{i_p} = \frac{n}{0.4463}\sqrt{\frac{RT}{F}}\sqrt{\frac{k[H^+]^2}{\nu}} = 0.72\sqrt{\frac{k[H^+]^2}{\nu}} \quad \textbf{(3)}$$

A = area of the electrode, D is the diffusion coefficient of the catalyst (D for the oxidised and reduced forms are assumed equal), n = 2 for H_2 production , R = 8.314 J/(mol K), F = 96485 C/mol, υ scan rate in V/s, k is the third order rate constant. Linearity of:

1. plots of i_{cat}/i_p vs acid concentration confirms that the electrocatalytic process is second order with respect to acid concentration

2. plots of i_{cat} vs [catalyst] confirms that the process is first order with respect to catalyst concentration

The rate law for the thirdorder process can be written as: $rate = k\,[H^+]^2\,[cat]$

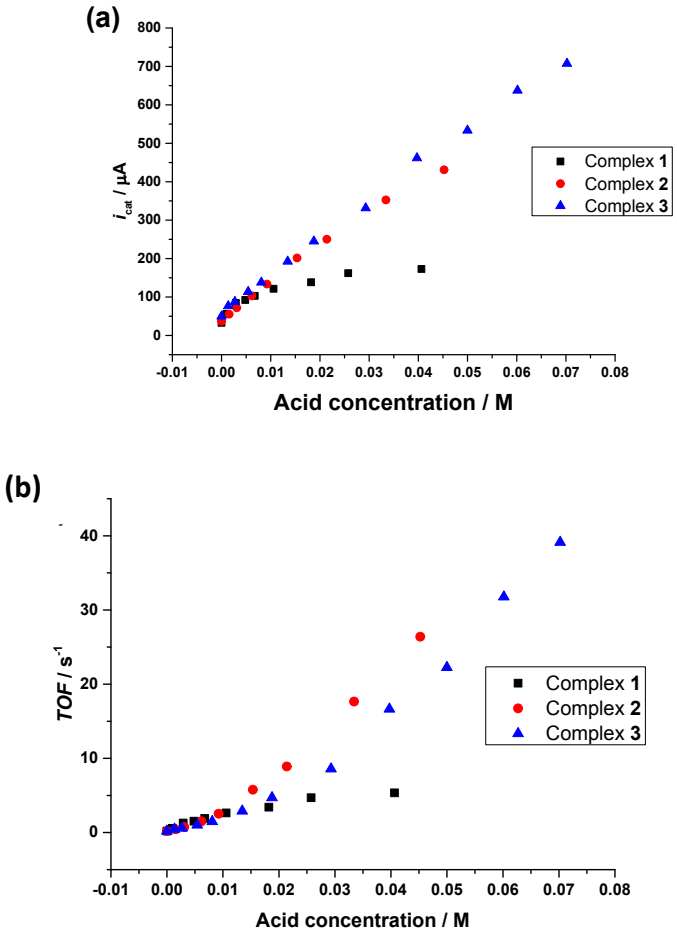

Figure S23. (a) i_{cat} vs acid concentration plot (negative sign for catalytic current has been ignored) and (b) k_{obs} (*TOF*, s^{-1}) vs acid concentration plot, (with acetic acid) for [^{iPr}POCOP^{iPr}]NiCl (**1**) (1 mM), for [^{iPr}POCSP^{iPr}]NiCl (**2**) (1.47 mM) and for [^{iPr}PSCSP^{iPr}]NiCl (**3**) (1.43 mM) in MeCN with 0.1 M TBAP at 0.1 V/s.

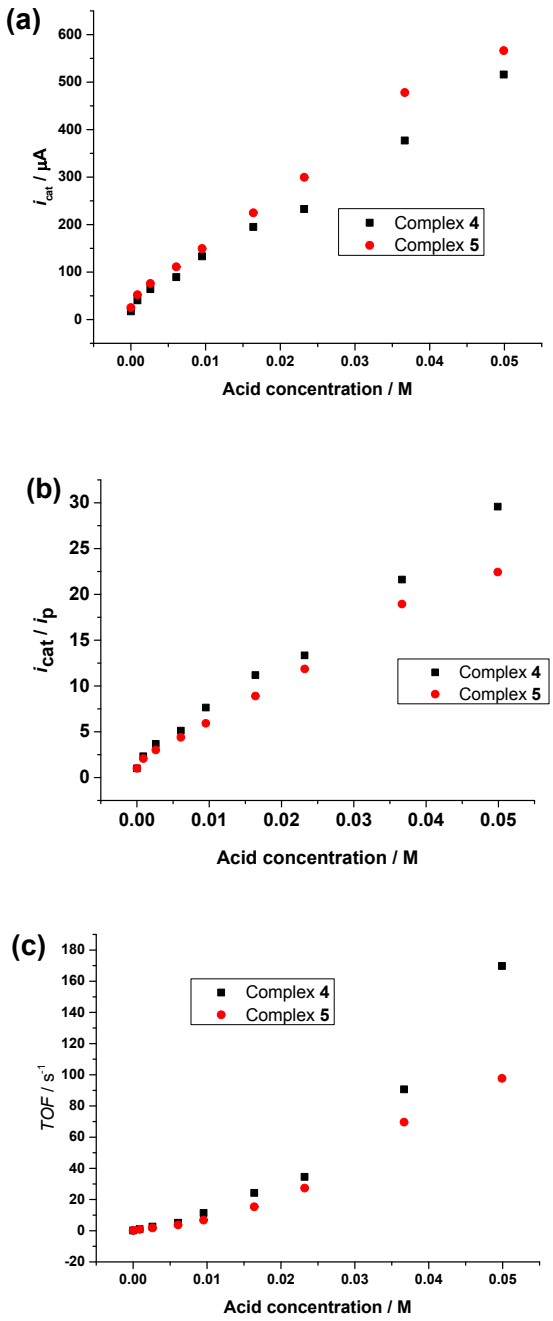

Figure S24. (a) i_{cat} vs acid concentration plot (negative sign for catalytic current has been ignored), (b) i_{cat} / i_p vs acid concentration (M) plots for [$^{i\text{Pr}}$POCOP$^{i\text{Pr}}$]NiSC$_6$H$_4$CH$_3$ (**4**) (1.15 mM) and for [$^{i\text{Pr}}$POCSP$^{i\text{Pr}}$]NiSC$_6$H$_4$CH$_3$ (**5**) (0.93 mM) (with acetic acid) and(c) k_{obs} (*TOF*, s^{-1}) vs acid concentration plot, (with acetic acid) for [$^{i\text{Pr}}$POCOP$^{i\text{Pr}}$]NiSC$_6$H$_4$CH$_3$ (**4**) (1.15 mM) and for [$^{i\text{Pr}}$POCSP$^{i\text{Pr}}$]NiSC$_6$H$_4$CH$_3$ (**5**) (0.93 mM) in MeCN with 0.1 M TBAP at 0.1 V/s.

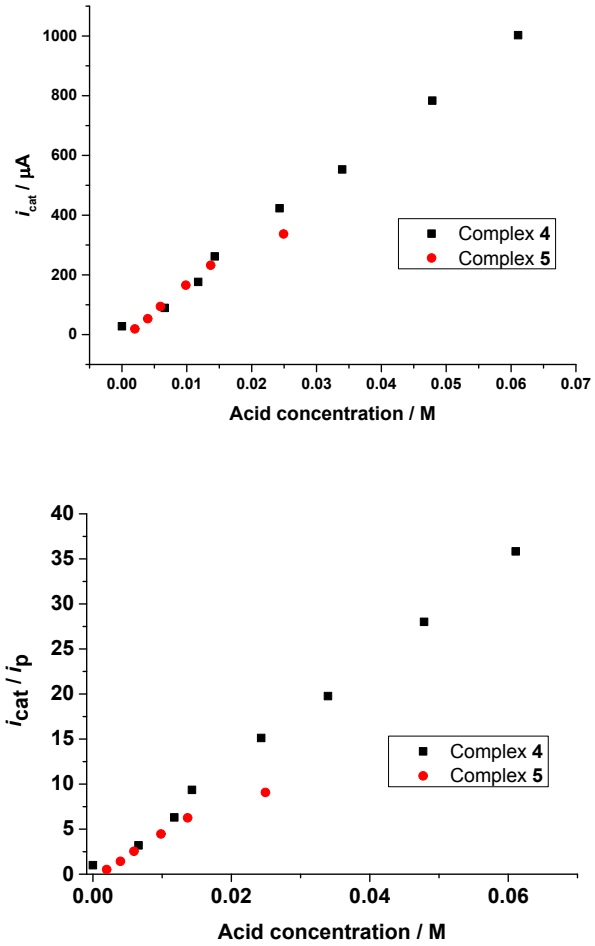

Figure S25. Top: i_{cat} vs acid concentration plot (with TFA) for [^{iPr}POCOP^{iPr}]NiSC$_6$H$_4$CH$_3$ (**4**) (0.85 mM) and for [^{iPr}POCSP^{iPr}]NiSC$_6$H$_4$CH$_3$ (**5**) (1.24 mM) in MeCN with 0.1 M TBAP at 0.1 V/s (negative sign for catalytic current has been ignored). Bottom: i_{cat} / i_p vs acid concentration (M) plot for [^{iPr}POCOP^{iPr}]NiSC$_6$H$_4$CH$_3$ (**4**) (0.85 mM) and for [^{iPr}POCSP^{iPr}]NiSC$_6$H$_4$CH$_3$ (**5**) (1.24 mM) (with TFA) in MeCN with 0.1 M TBAP at 0.1 V/s.

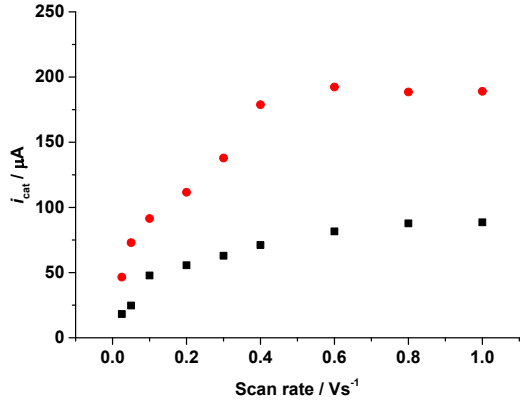

Figure S26. Plot of i_{cat} (μA) vs. scan rate (Vs^{-1}) for complex [$^{i\text{Pr}}$POCOP$^{i\text{Pr}}$]NiCl (**1**) (0.5 mM) with 2.61 mM (■) and 9.53 mM (●) acetic acid in 0.1 M [NBu_4][PF_6] / MeCN. Negative sign for catalytic current has been ignored.

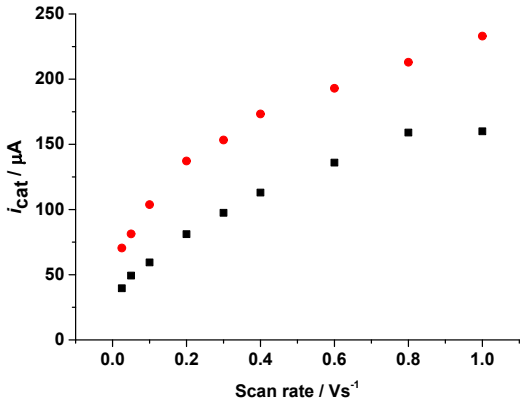

Figure S27. Plot of i_{cat} (μA) vs. scan rate (Vs^{-1}) for complex [$^{i\text{Pr}}$POCSP$^{i\text{Pr}}$]NiCl (**2**) (1.11 mM) with 1.74 mM (■) and 4.52 mM (●) acetic acid in 0.1 M [NBu_4][PF_6] / MeCN. Negative sign for catalytic current has been ignored.

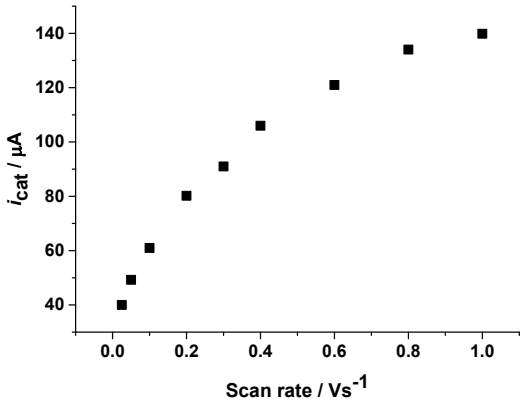

Figure S28. Plot of (a) i_{cat} (μA) vs. scan rate (Vs^{-1}) for complex [$^{i\text{Pr}}$PSCSP$^{i\text{Pr}}$]NiCl (**3**) (1.07 mM) with 3.48 mM (■) acetic acid in 0.1 M [NBu_4][PF_6] / MeCN. Negative sign for catalytic current has been ignored.

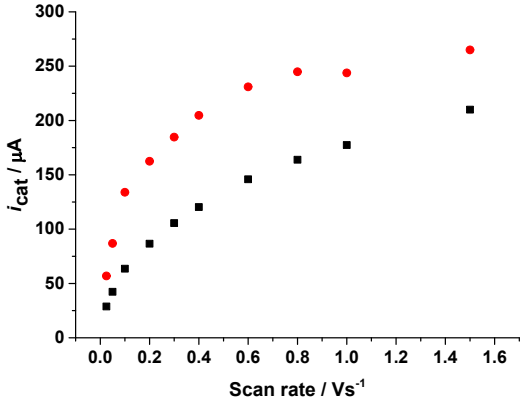

Figure S29. Plot of i_{cat} (μA) vs. scan rate (Vs^{-1}) for complex [$^{i\text{Pr}}$POCOP$^{i\text{Pr}}$]NiSC$_6$H$_4$CH$_3$ (**4**) (1.15 mM) with 2.61 mM (■) and 9.53 mM (●) acetic acid in 0.1 M [NBu$_4$][PF$_6$] / MeCN. Negative sign for catalytic current has been ignored.

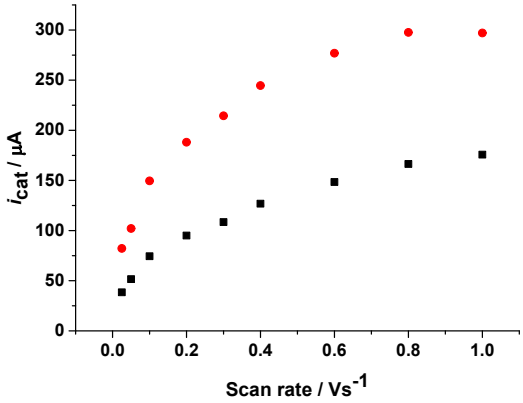

Figure S30. Plot of i_{cat} (μA) vs. scan rate (Vs^{-1}) for complex [$^{i\text{Pr}}$POCSP$^{i\text{Pr}}$]NiSC$_6$H$_4$CH$_3$ (**5**) (0.93 mM) with 2.61 mM (■) and 9.53 mM (●) acetic acid in 0.1 M [NBu$_4$][PF$_6$] / MeCN. Negative sign for catalytic current has been ignored.

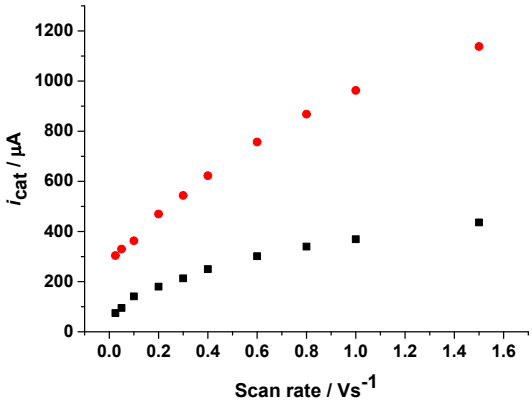

Figure S31. Plot of i_{cat} (µA) vs. scan rate (Vs^{-1}) for complex [^{iPr}POCOP^{iPr}]$NiSC_6H_4CH_3$ (**4**) (1.5 mM) with 4.17 mM (■) and 13.5 mM (●) TFA in 0.1 M [NBu_4][PF_6] / MeCN. Negative sign for catalytic current has been ignored. No kinetic information can be extracted in these experiments since a region independent of scan rate was not fully reached.

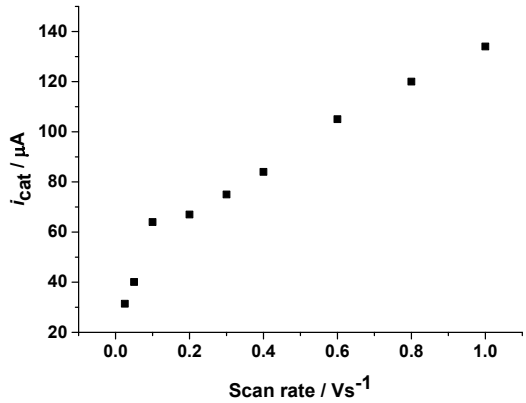

Figure 32. Plot of i_{cat} (µA) vs. scan rate (Vs^{-1}) for complex [^{iPr}POCSP^{iPr}]$NiSC_6H_4CH_3$ (**5**) (1.24 mM) with 3.97 mM (■) TFA in 0.1 M [NBu_4][PF_6] / MeCN. Negative sign for catalytic current has been ignored. No kinetic information can be extracted in these experiments since a region independent of scan rate was not fully reached.

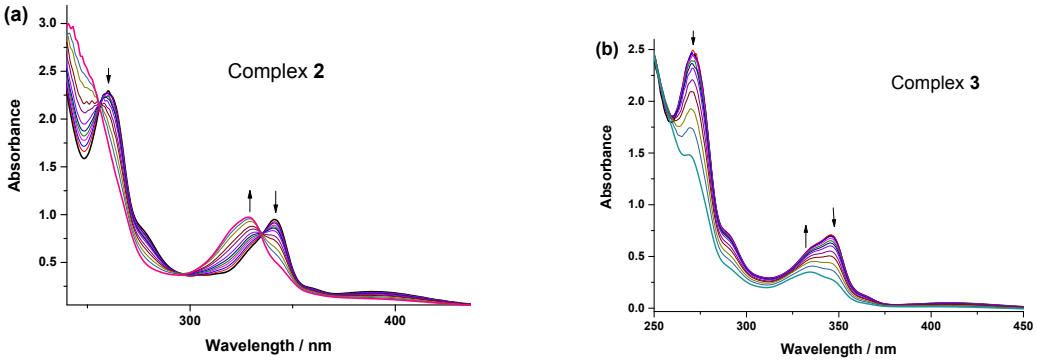

Figure S33. UV-Vis absorption spectroscopy (l = 1 mm) of (a) complex [$^{i\text{Pr}}$POCSP$^{i\text{Pr}}$]NiCl (**2**) (0.18 mM) and (b) complex [$^{i\text{Pr}}$PSCSP$^{i\text{Pr}}$]NiCl (**3**) (0.09 mM) recorded in acetonitrile under different concentrations of TFA (0-93 mM). The spectral changes upon addition of increasing amounts of acid are indicated by arrows.

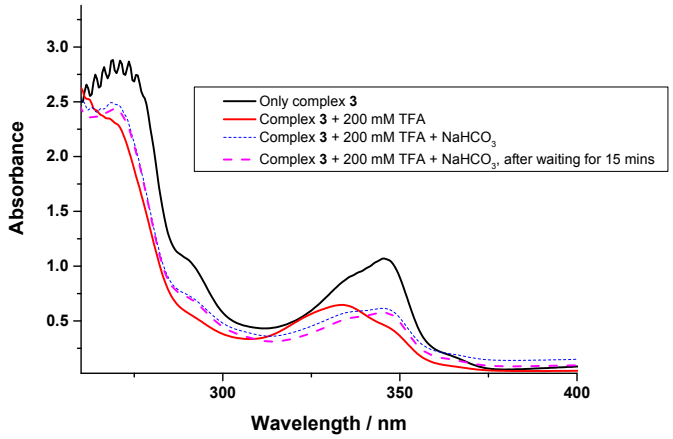

Figure S34. UV-Vis experiments in acetonitrile for [$^{i\text{Pr}}$PSCSP$^{i\text{Pr}}$]NiCl (**3**) in the absence and presence of TFA and after addition of $NaHCO_3$.

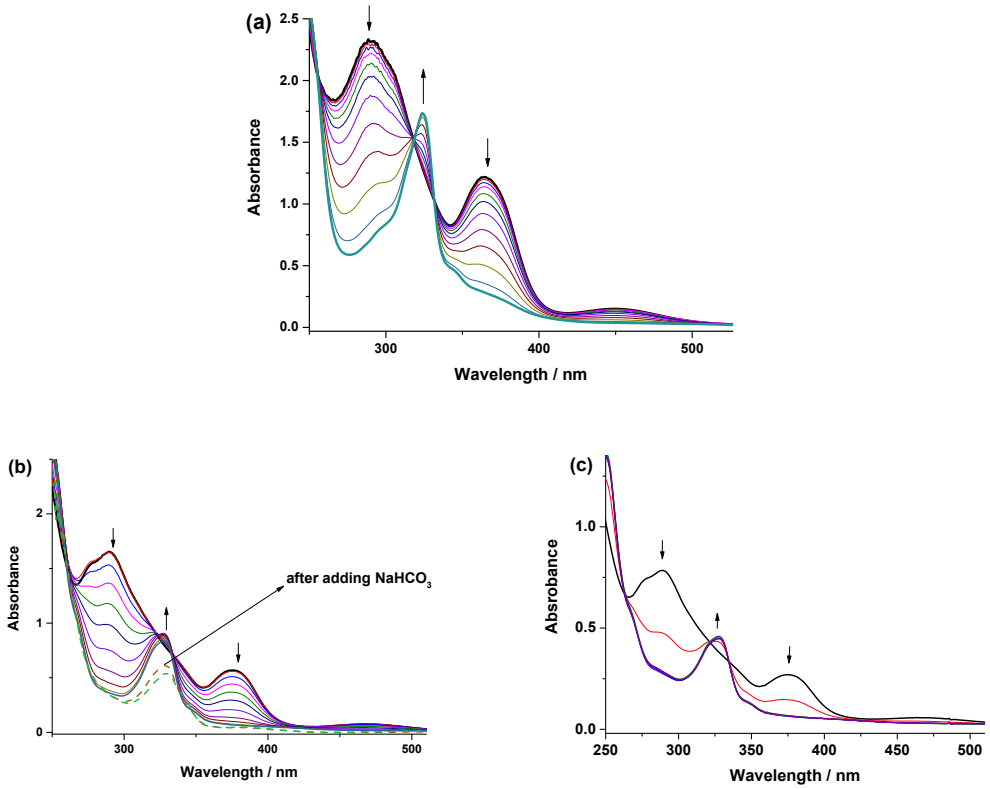

Figure S35. UV-Vis absorption spectroscopy (l = 1 mm) recorded in acetonitrile for complexes (a) [$^{i\text{Pr}}$POCOP$^{i\text{Pr}}$]NiSC$_6$H$_4$CH$_3$ (**4**) (0.25 mM) under different concentrations of acetic acid (0-580 mM) and (b) [$^{i\text{Pr}}$POCSP$^{i\text{Pr}}$]NiSC$_6$H$_4$CH$_3$ (**5**) (0.15 mM) under different concentrations of acetic acid (0-1160 mM). The dotted lines represent the UV-Vis measurements after addition of $NaHCO_3$ to the acetonitrile solution and (c) [$^{i\text{Pr}}$POCSP$^{i\text{Pr}}$]NiSC$_6$H$_4$CH$_3$ (**5**) (0.10 mM) under different concentrations of TFA (0-5 mM). The spectral changes upon addition of increasing amounts of acid are indicated by arrows.

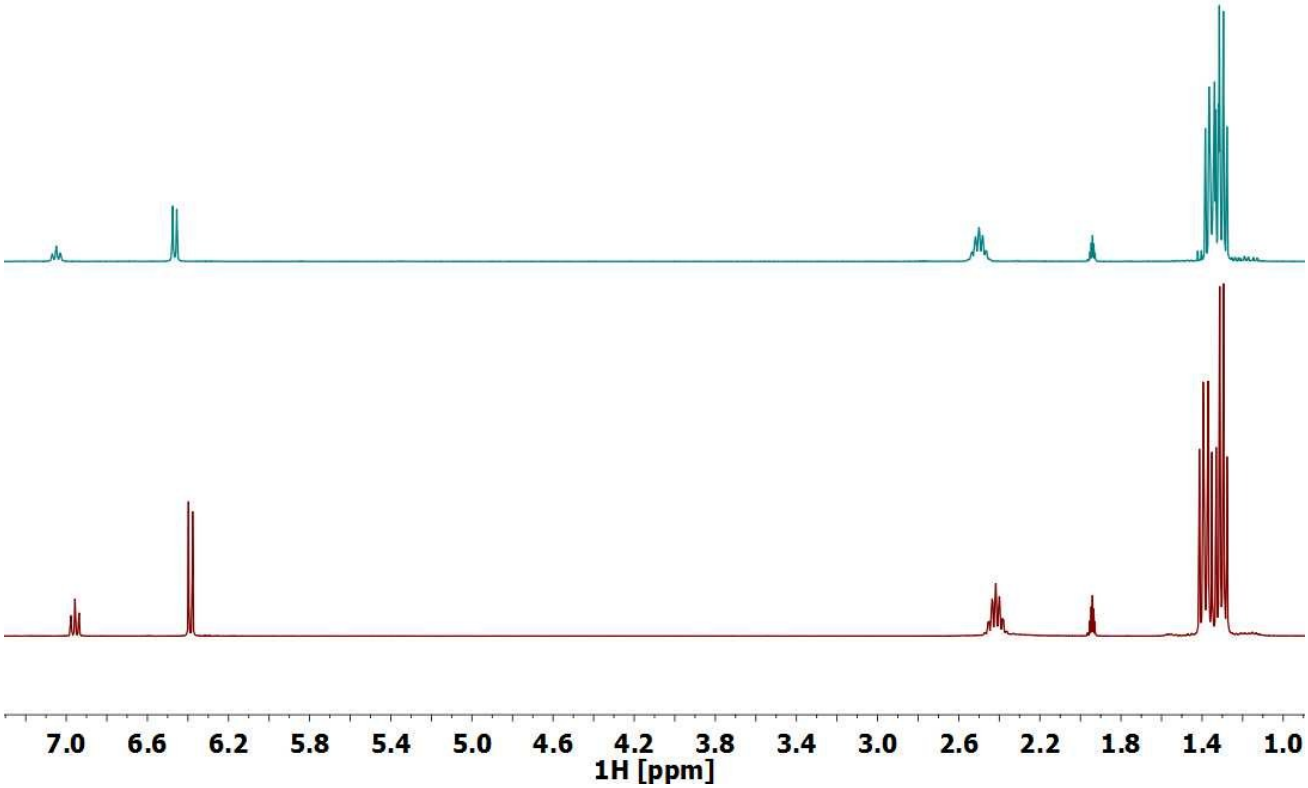

Figure S36. ^{1}H NMR spectra for [$^{i\text{Pr}}$POCOP$^{i\text{Pr}}$]NiCl (**1**) in CD_3CN without (red) and with (green) TFA.

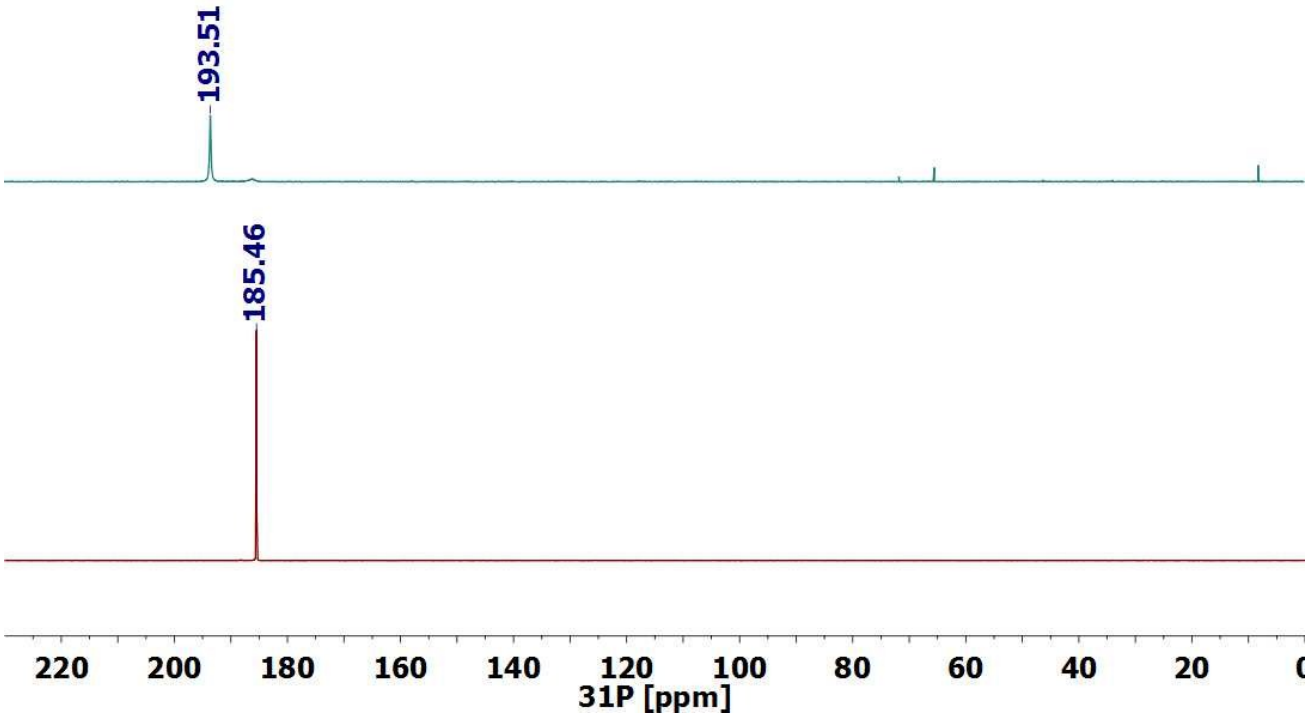

Figure S37. $^{31}P\{^{1}H\}$NMR spectra for [$^{i\text{Pr}}$POCOP$^{i\text{Pr}}$]NiCl (**1**) in CD_3CN without (red) and with (green) TFA.

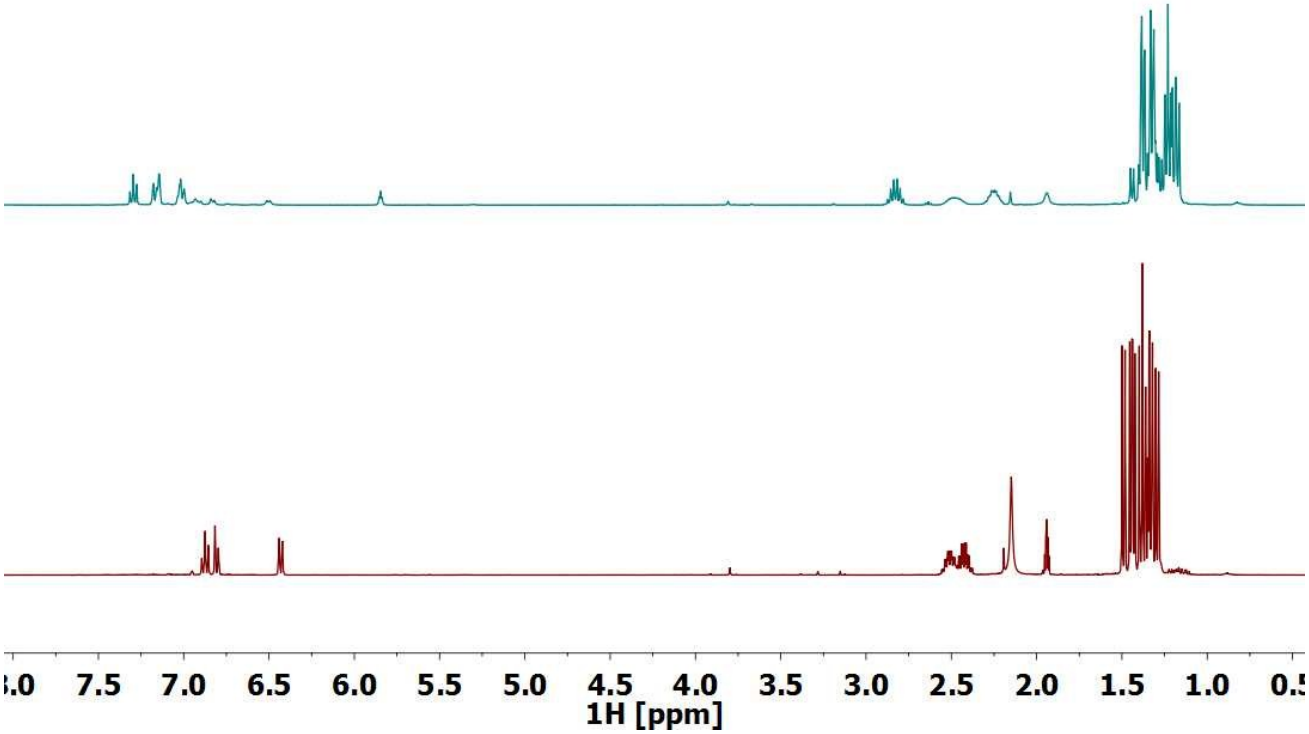

Figure S38. ^{1}H NMR spectra for [$^{i\text{Pr}}$POCSP$^{i\text{Pr}}$]NiCl (**2**) in CD_3CN without (red) and with (green) TFA.

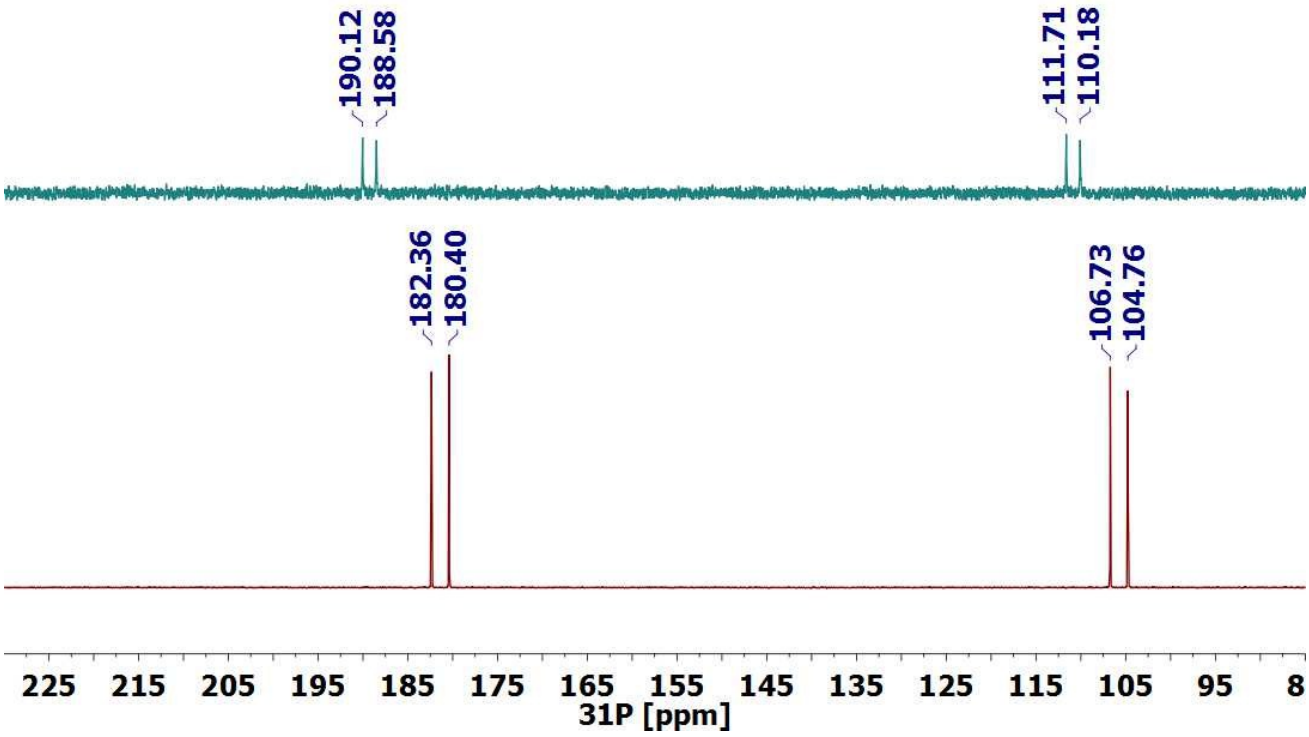

Figure S39. $^{31}P\{^{1}H\}$ NMR spectra for [$^{i\text{Pr}}$POCSP$^{i\text{Pr}}$]NiCl (**2**) in CD_3CN without (red) and with (green) TFA.

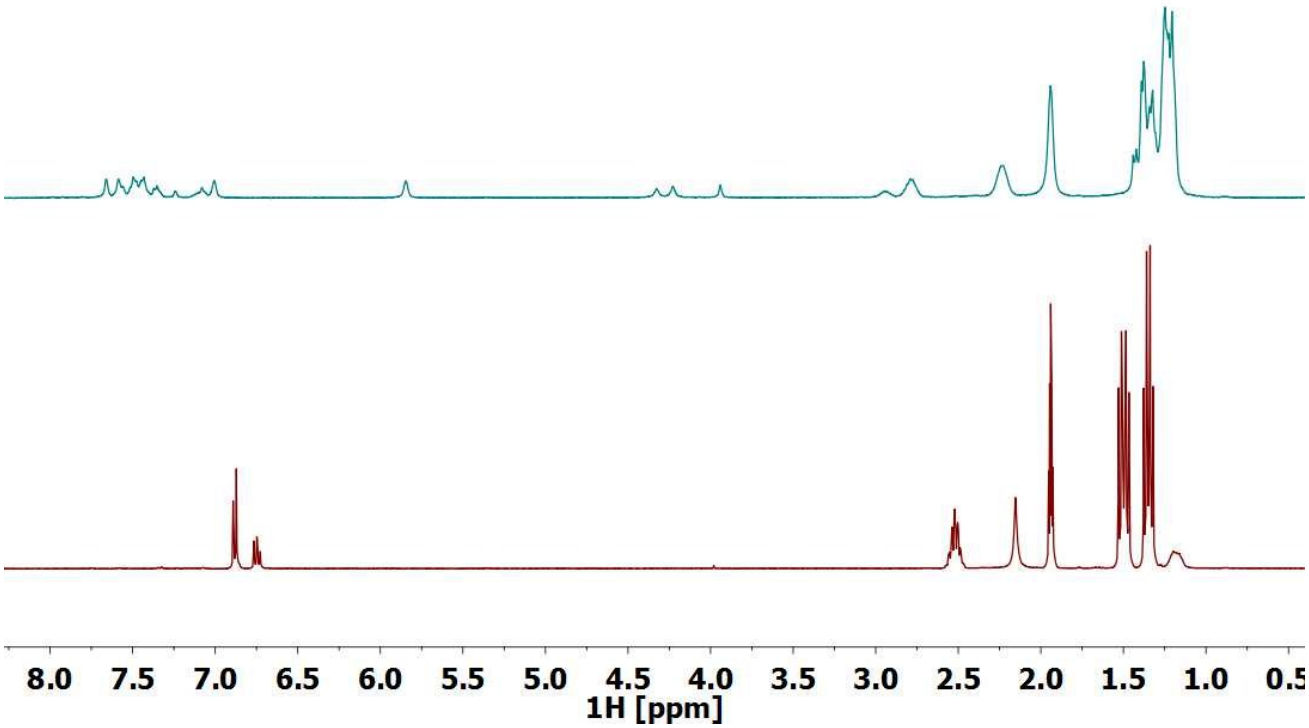

Figure S40. ^{1}H NMR spectra for [$^{i\text{Pr}}$PSCSP$^{i\text{Pr}}$]NiCl (**3**) in CD_3CN without (red) and with (green) TFA.

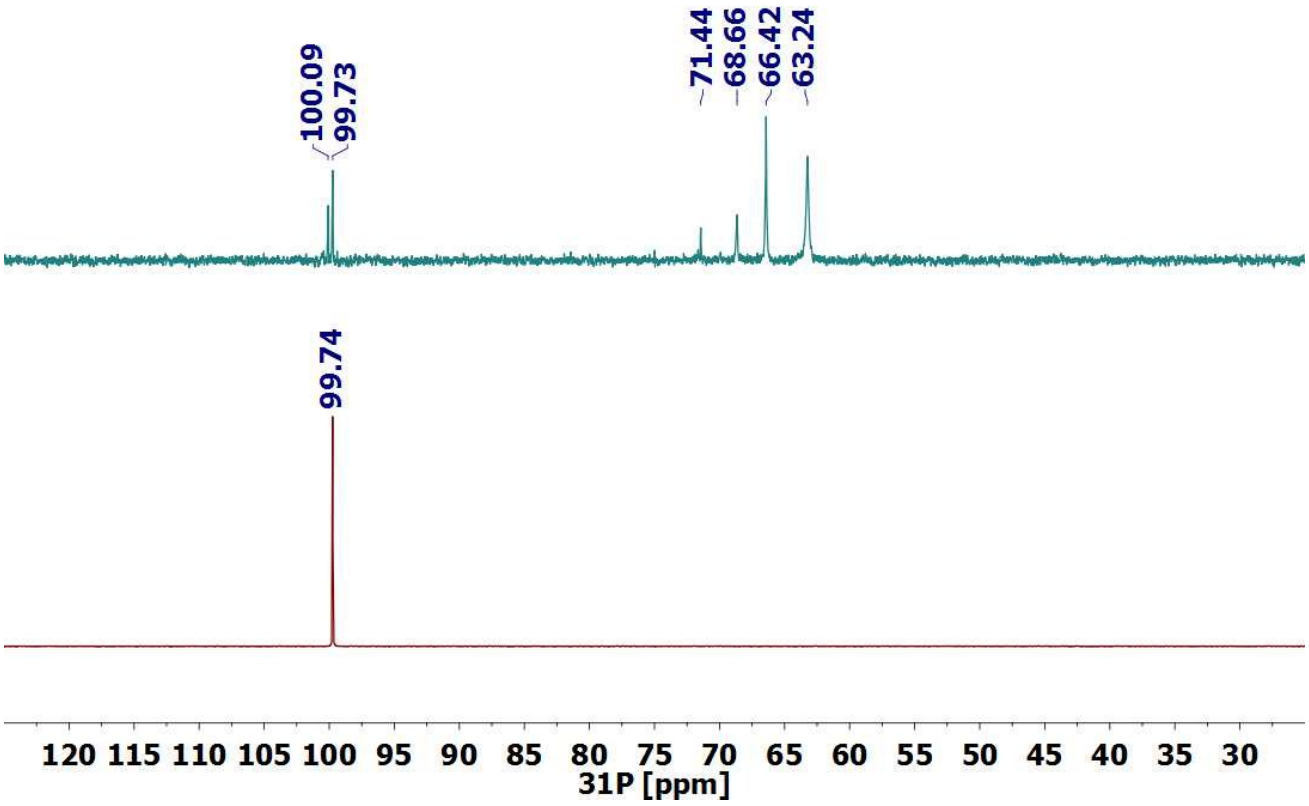

Figure S41. $^{31}P\{^{1}H\}$ NMR spectra for [$^{i\text{Pr}}$PSCSP$^{i\text{Pr}}$]NiCl (**3**) in CD_3CN without (red) and with (green) TFA.

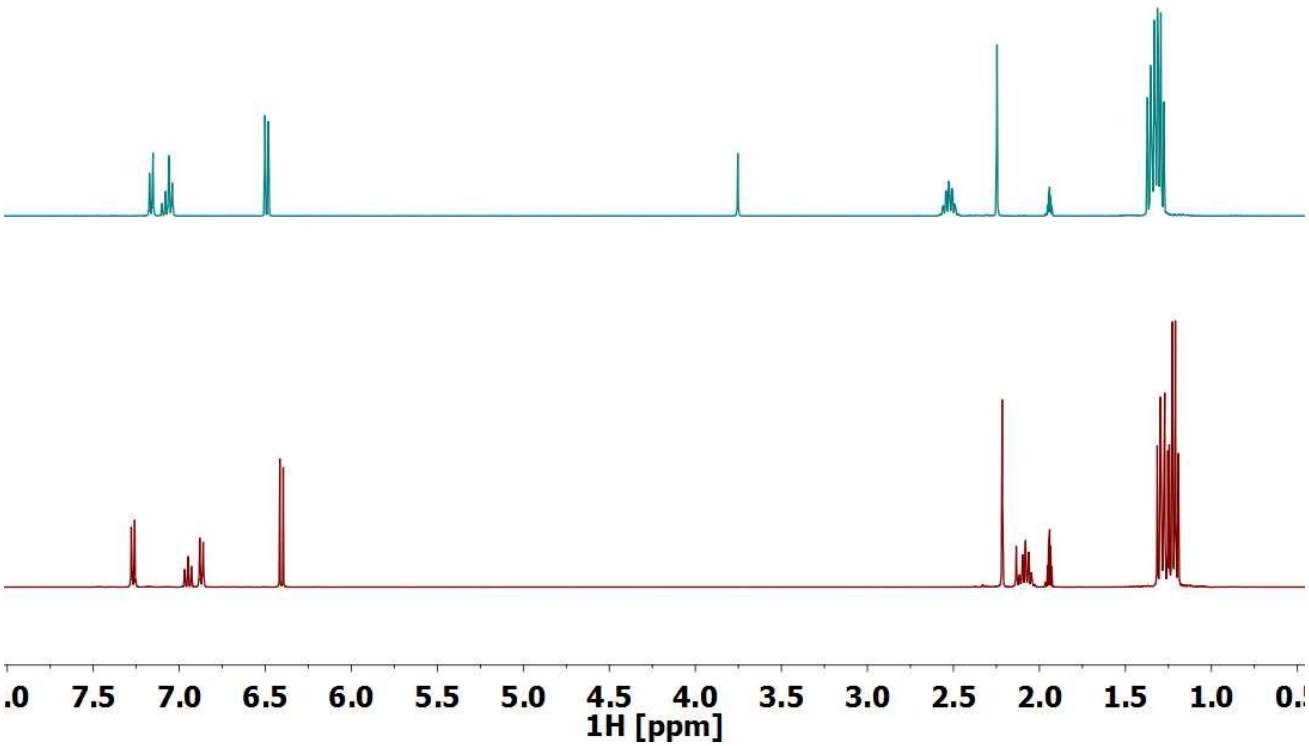

Figure S42. ^{1}H NMR spectra for [$^{i\text{Pr}}$POCOP$^{i\text{Pr}}$]NiSC$_6$H$_4$CH$_3$ (**4**) in CD$_3$CN without (red) and with (green) TFA.

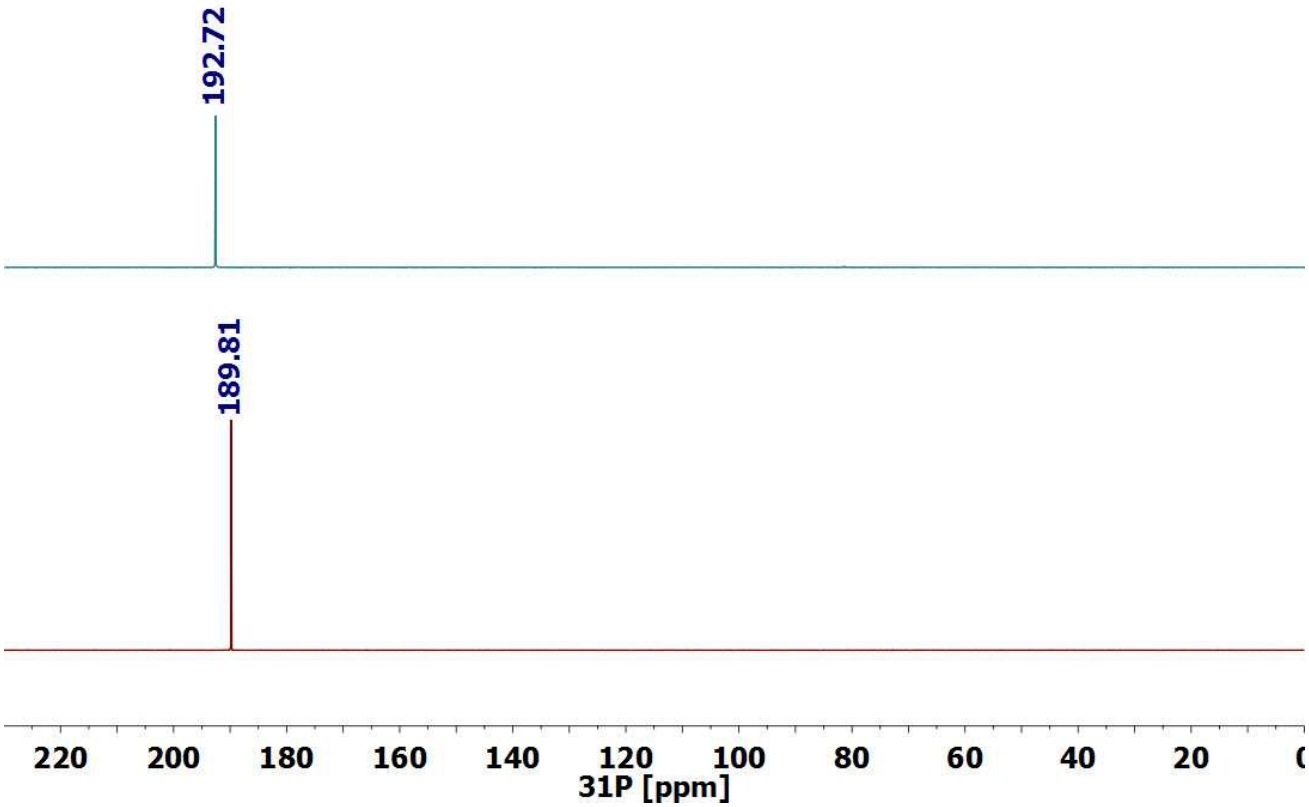

Figure S43. $^{31}P\{^{1}H\}$ NMR spectra for [$^{i\text{Pr}}$POCOP$^{i\text{Pr}}$]NiSC$_6$H$_4$CH$_3$ (**4**) in CD$_3$CN without (red) and with (green) TFA.

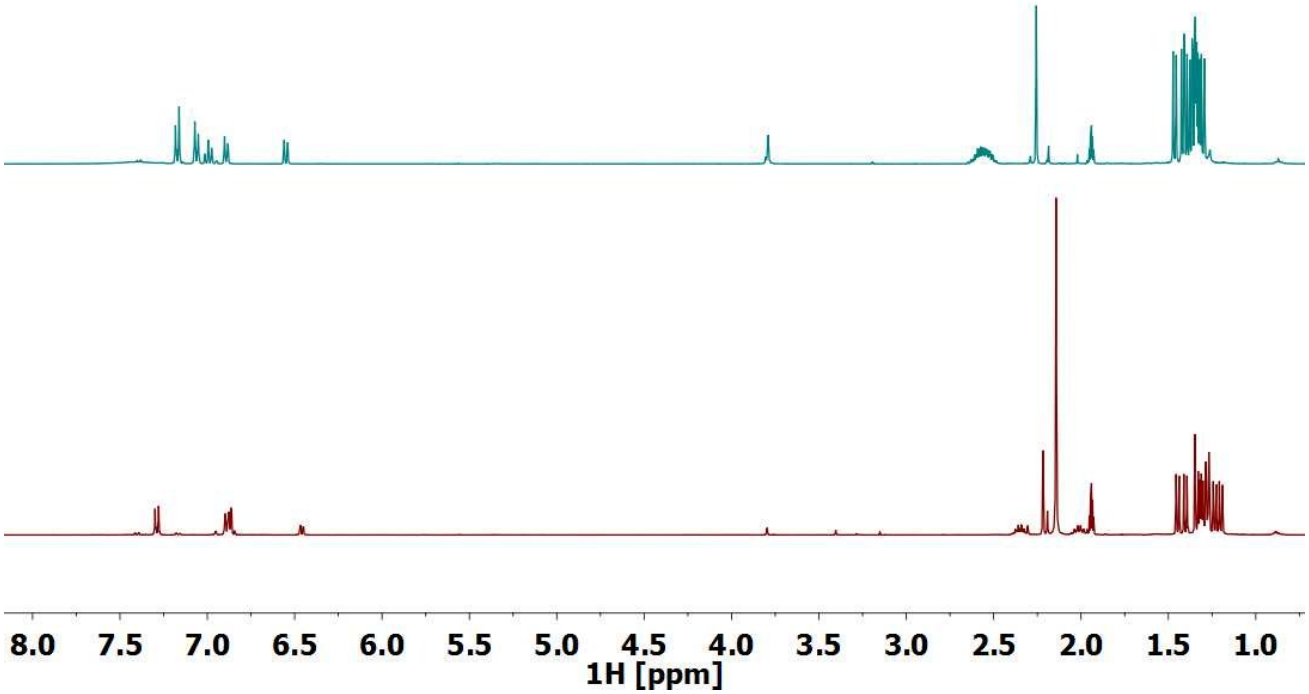

Figure S44. ^{1}H NMR spectra for [$^{i\text{Pr}}$POCSP$^{i\text{Pr}}$]NiSC$_6$H$_4$CH$_3$ (**5**) in CD_3CN without (red) and with (green) TFA.

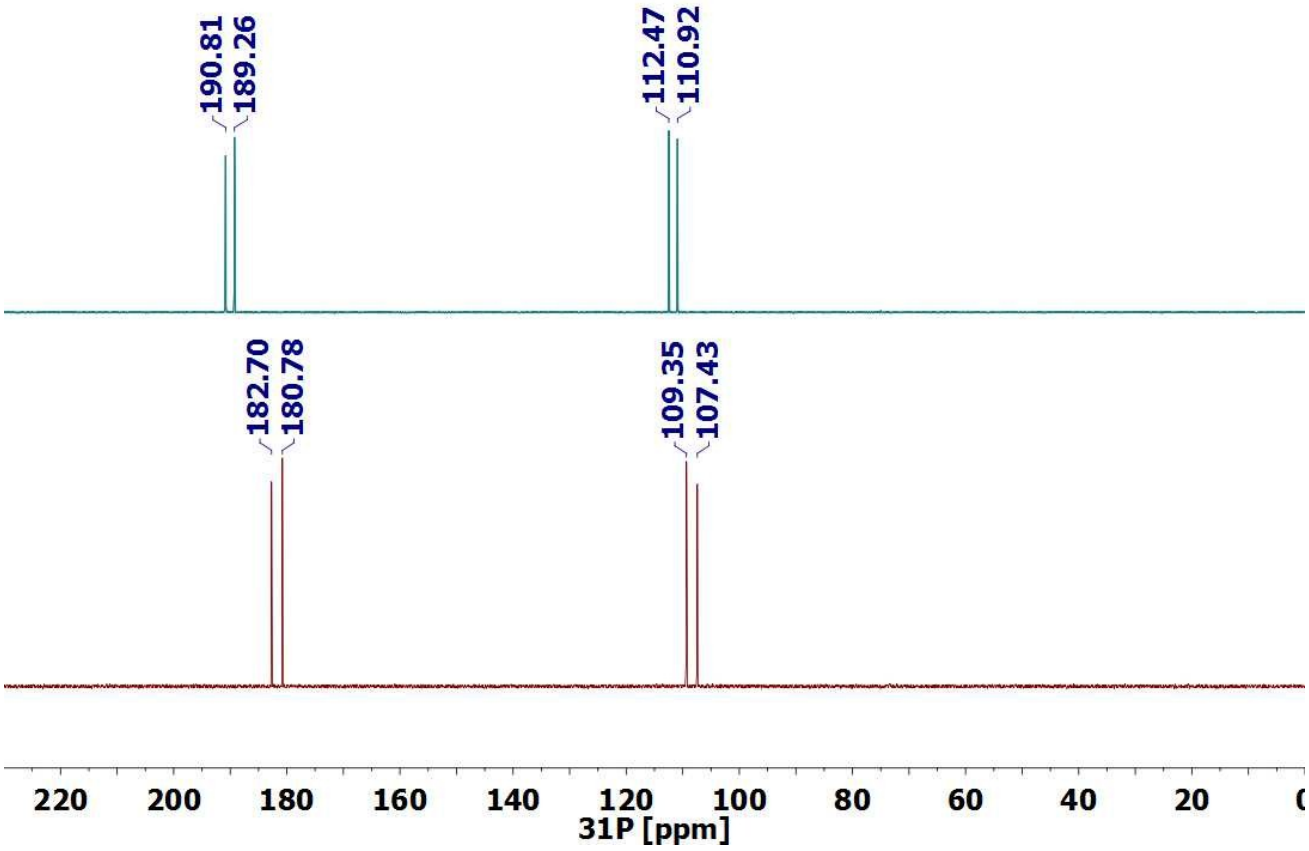

Figure S45. $^{31}P\{^{1}H\}$ NMR spectra for [$^{i\text{Pr}}$POCSP$^{i\text{Pr}}$]NiSC$_6$H$_4$CH$_3$ (**5**) in CD_3CN without (red) and with (green) TFA.

Table S1. Crystallographic parameters for complex **6**.

	[$^{i\text{Pr}}$PSCSP$^{i\text{Pr}}$]NiSC$_6$H$_4$CH$_3$ (6)
Chemical formula	$C_{25}H_{38}NiP_2S_3$
Formula weight	555.38 g/mol
Colour	red
Crystal system	monoclinic
Space group	*C*2/*c*
Unit cell dimensions	
a, b, c	30.1685(9) Å 9.1638(3) Å 20.4900(6) Å
α, β, γ	90° 105.7342(11)° 90°
Cell volume	5452.4(3) Å^3
Z	8
Temperature	150(2) K
Wavelength	0.7107 Å (Mo-K_α)
Reflections collected	63008
Independent reflections	6581
Observed reflections (I > 2σ(I))	5819
Parameters	289
GOF (F^2)	1.038
R_1 (I > 2σ(I))	0.0266
wR_2 (all data)	0.0698

Qualitative Analysis Report

Instrument Name	LCMS	**Data Filename**	D:\Chem32\1\Data\1901\19012905.D
Acq Method	100%ACN - SCAN Pos	**Sample Name**	PH 158
DA Method	HRMS.m	**Position**	Vial 21
User Name	SYSTEM	**Comment**	ACN

User Spectra

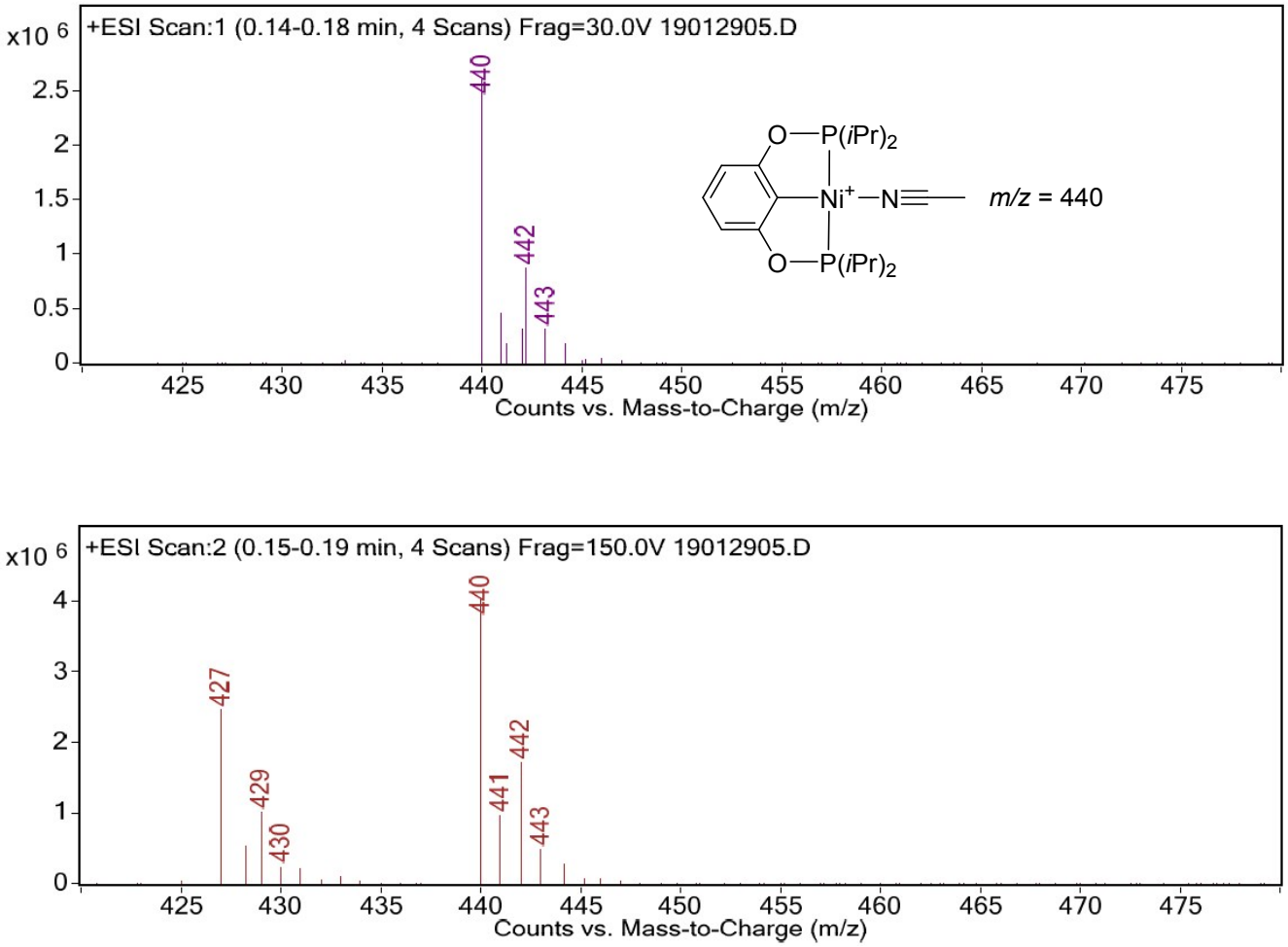

Figure S46. LC-MS spectra (low resolution) for complex **1** in MeCN with 10 equiv. of TFA added.

Elemental Composition Report

Hasche PH 159

Mass	Calc. Mass	mDa	PPM	Formula
456.1184	456.1190	-0.6	-1.3	C20 H34 N O P2 S Ni

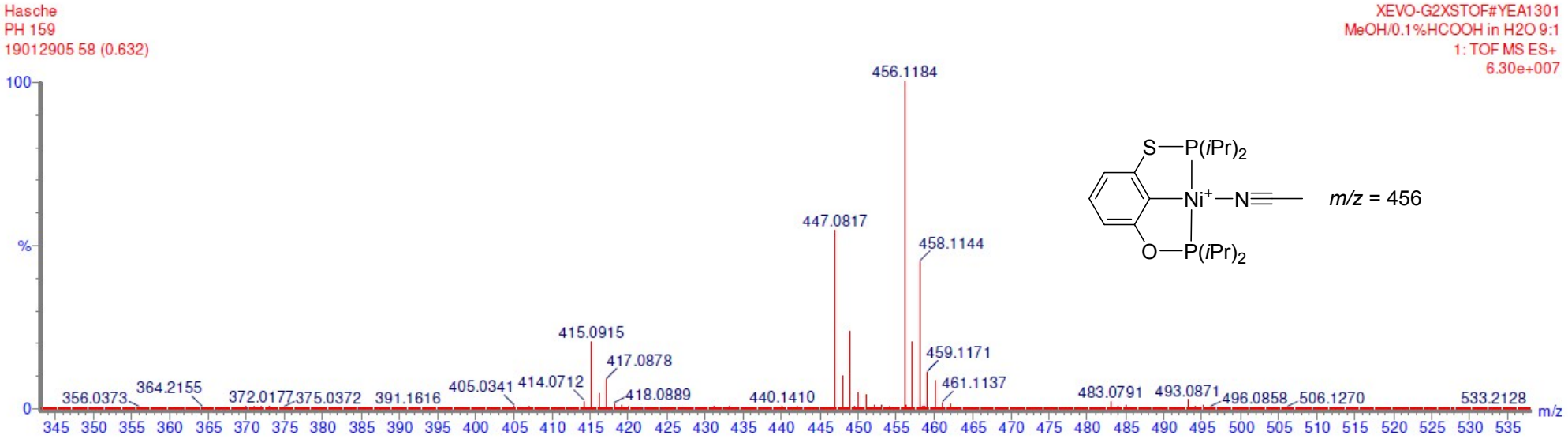

Figure S47. LC-MS spectrum (high resolution) for complex **2** with 10 equiv. of TFA added.

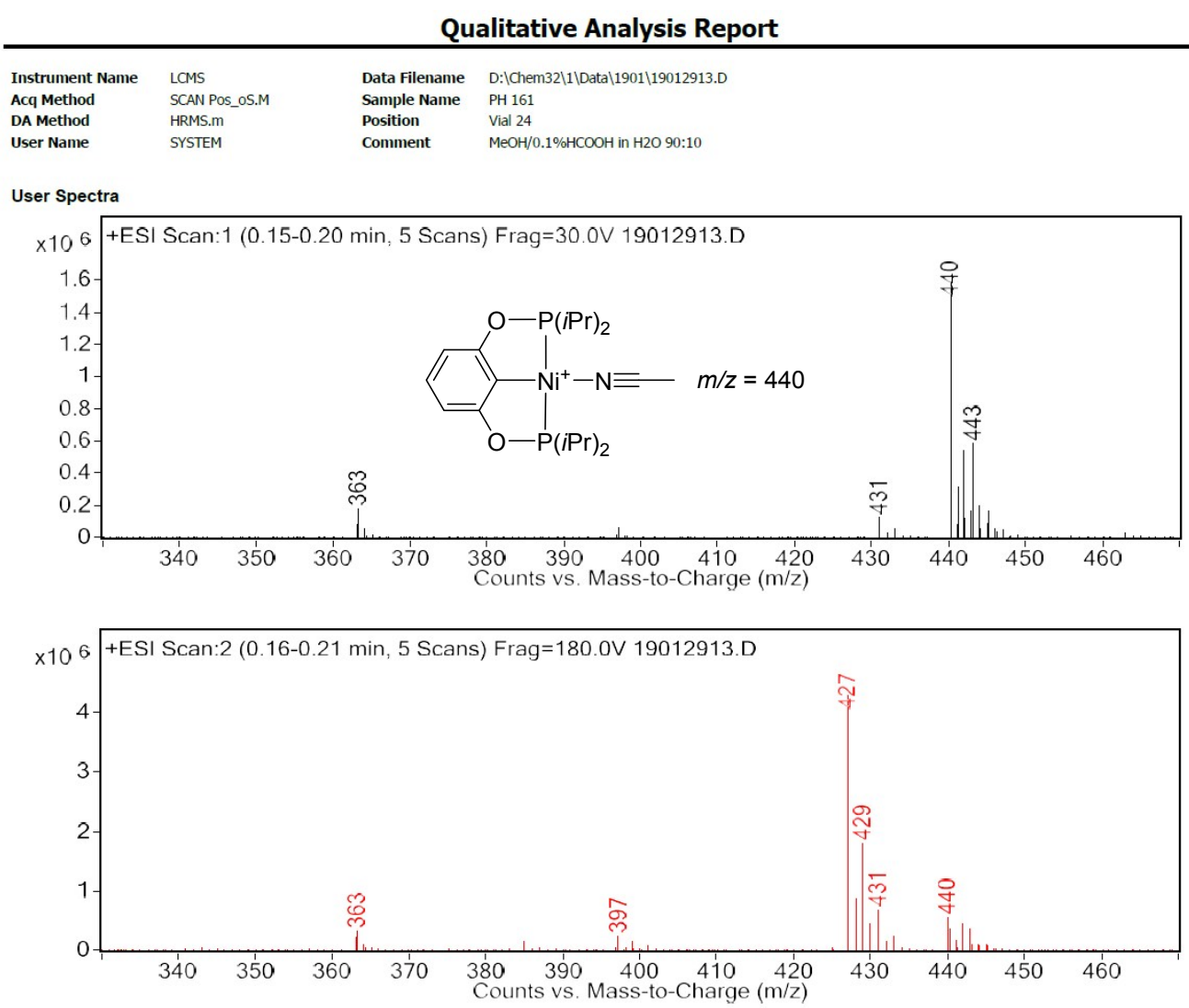

Figure S48. LC-MS spectra (low resolution) for complex **4** with 10 equiv. of TFA added.